1. General

This alloy was developed in the early 1970's by RMI Company under an Air Force Contract. The goal was to produce a composition which had higher hardenability than available α-β titanium alloys (e.g. Ti-6Al-4V) coupled with improved strength and good fracture toughness. By appropriate balance of the beta stabilizer elements Cr and Mo coupled with a small silicon addition, these goals were largely achieved. The resulting alloy had a modulus somewhat higher than widely used 6Al-4V. In 1988-1989 there was renewed interest in the alloy for applications in advanced military aircraft. Interest in these applications led to refinements in the composition and the development of thermomechanical processes designed to produce optimum combinations of strength and toughness. This Chapter presents both the old data and that resulting from recent investigations.

1.1 Commercial Designations

Ti-6Al-2Zr-2Mo-2Cr, Ti-6-2-2-2-2.

1.2 Alternate Designations

Ti-6-22-22, Ti-6-22-22Si, Ti-6Q2.

1.3 Specifications

1.3.1 *[Table]* Proposed design mechanical property values for α-β processed forgings and plate.

1.4 Composition

1.4.1 *[Table]* Chemical composition.

1.5 Heat Treatment

General. A range of mechanical properties can be developed by thermal-mechanical processes (TMP) which involve the interactive effect of forging conditions and subsequent heat treatment. The TMP determines the microstructure which in turn influences the mechanical properties in a complex manner.

Terminology. The following terminology is used when referring to the various steps in the TMP:

Finish forge temperature: the final soak temperature used prior to the last forging operation. Depending on the forging size and process, the part temperature will usually drop from the soak temperature during forging.

Beta forging: the finish forge temperature is above the beta transus (β_t) and the majority of the work is performed above β_t. This is sometimes referred to as through transus forging.

Alpha-beta forging: the final soak temperature is below the beta transus and the finish forge temperature is below the beta transus.

Beta solution treat: the solution temperature is above the beta transus.

This section produced with the support of NASA-Lewis Research Center.

© 1995 by Purdue Research Foundation, West Lafayette, Indiana 47907. All Rights Reserved. U.S. Government License. This material may be used, duplicated or disclosed by United States Government agencies without the payment of any royalty.

Ti
6 Al
2 Sn
2 Zr
2 Mo
2 Cr
0.2 Si

Subtransus solution treat: the solution temperature is below the beta transus. This is sometimes referred to as an α-β heat treatment.

Conventional processing: finish forging below the beta transus followed by a single step subtransus solution treatment and aging at 1000F. This was the original processing schedule.

Mill anneal: 1350 to 1450F.

Duplex anneal: a two step subtransus solution treatment applied to α-β finished forging and plate used in some early development work.

Triplex heat treatment: a two step solution heat treatment where temperature in the first step is above the beta transus followed by rapid cooling to a subtransus temperature, air cooling and aging. This is presently the preferred heat treatment.

Effects of the TMP. It is obvious from the above that a wide range of microstructures and associated mechanical properties can be obtained from variations in the TMP. The majority of early data corresponded to α-β finish forging followed by a sub beta transus solution treatment (see Table 1.5.1.1). This TMP produced high strengths but relatively low fracture toughness.

A limited amount of the early data was produced using a duplex anneal of 1740F, AC to 1560F, WQ + 1000F, age.

More recently, studies of the effects of TMP variables have indicated that improved mechanical properties are associated with a transformed beta microstructure of acicular alpha containing little or no grain boundary alpha (Refs. 4, 6, 20). Data relating to one of these studies are summarized in Tables 1.5.1.1 and 1.5.1.2. The best combination of tensile properties and fracture toughness were produced by beta finish forging followed by solution treating somewhat below the beta transus and aging at 1000F (see Table 1.5.1.1, processes 1 and 2). The resulting microstructure was lamellar alpha with little or no grain boundary alpha. Alpha-beta finish forging followed by subtransus solution treating and aging at 1000F (see Table 1.5.1.1, processes 3 and 4) produced tensile strengths about equal to those resulting from beta finish forging but substantially reduced fracture toughness. The resulting microstructures consisted primarily of broken lamellar with equiaxed primary alpha. Processess 5 and 6 combine alpha-beta finish forging with a beta solution treatment. Process 6 employed a two step solution treatment producing tensile strengths and fracture toughness values nearly equal to those obtained by finish forging above the beta transus. This latter heat treatment is sometimes referred to as a triplex treatment. It has the advantage of producing desirable combinations of tensile strengths and fracture toughness without the very careful control of the forging process required by beta finish forging. The resulting microstructure was characterized by relatively coarse acicular alpha (Widmanstaten type). A triplex treatment is presently recommended (see Table 1.5.1.3) for forgings used in critical applications.

Highly acicular transformed microstructures would be expected to possess superior fatigue crack propagation resistance due to energy absorption associated with crack front splitting (Ref. 5). However, fatigue crack propagation data (see Figures 3.5.3.6 and 3.5.3.7) obtained for three TMPs did appear to correlate with the acicularity of the alpha platelets as judged from the TMP applied.

Cooling rate. The cooling rate from the solution treatment can alter the mechanical properties with the faster rates providing the higher tensile strengths. This cooling rate effect may be seen by comparing the tensile strengths and fracture toughness for the pancake and closed die forgings in Table 1.5.1.2. The fan cooled material had somewhat lower tensile strengths but higher fracture toughness than the oil quenched forging. The acicular alpha platelets increase in size with decrease in the cooling rate (Ref. 20). Another cooling rate study (see Figure 1.5.1.4) illustrated the variation of tensile strength with several quench methods from a subtransus solution temperature following beta finish forging (Ref. 20). As might be expected, the tensile strength falls with decreasing cooling rate which results in an increasing broadening of the alpha platelets. It appears that adequate fan cooling from the solution temperature can produce through hardening in section sizes up to three inches.

There is no assurance that a single TMP process can be defined as optimum for all forms of the alloy. However, based on available information, the triplex heat treatment shown in Table 1.5.1.3 is recommended for forgings and plates that have been alpha-beta finished forged.

1.5.1 Conventional Processing. Finish forge 1650 to 1700F + 1600 to 1700F, 0.5 hr, AC + 900 to 100F.

1.5.1.1 *[Table]* Effect of thermal mechanical processing on the tensile properties and fracture toughness of pancake forgings.

1.5.1.2 *[Table]* Effect of several thermal mechanical processes on the tensile properties and fracture toughness of forgings.

1.5.1.3 *[Table]* Triplex heat treatments specified for α-β finished forgings and plate.

1.5.1.4 *[Figure]* Effect of cooling rate on the tensile strength of a forging.

1.6 Hardness

Mill annealed – 39 RC.
α-β forged and triplex heat treated – 41-42 RC.

1.7 Forms and Conditions Available

Billets, forgings, plate, sheet and weld wire.

1.8 Melting and Casting Practice

1.9 Special Considerations

1.9.1 Effects of Silicon. The additions of Si increase the creep resistance of α-β titanium alloys and also increase the tensile strength. However, silicides of the form $(Ti,Zr)_5Si_3$ can precipitate at prior β grain boundaries and/or α-β platelet interfaces. This precipitation occurs on slow cooling from the solution temperature. These precipitates can substantially reduce the tensile ductility and the fracture toughness.

Recent work (Ref. 24) has systematically explored the influence of silicon on the tensile properties and fracture toughness of laboratory produced plate given several heat treatments. The results of this investigation are shown in Tables 1.9.1.1 through 1.9.1.3. For the triplex heat treatment (see Table 1.9.1.1) a substantial increase in tensile strength and a corresponding reduction in fracture toughness results from increasing the silicon level from 0.03 to 0.30 percent at an Oe of 0.18. Approximate TTT diagrams at different silicon levels indicate the maximum precipitation occurs between 1450 to 1500F. The deleterious effect of slow cooling through this temperature range is illustrated by the data in Table 1.9.1.2, which represent an intermediate hold at 1500F prior to aging. The result is low fracture toughness with the highest silicon level producing predominately intergranular fracture.

A regression analysis was used in an attempt to separate the effects of silicon from that of oxygen equivalent. The effect of silicon from this analysis was represented by the following expressions:

$$F_{ty} = 137.5 + 36.3 \text{ percent Si}$$
$$RA = 15.5 - 6.1 \text{ percent Si}$$
$$F_{tu} = 158.5 + 49.2 \text{ percent Si}$$
$$K_{Ic} = 91.6 - 49.5 \text{ percent Si.}$$

Increasing the aging temperature to 1150F (see Table 1.9.1.3) produced substantial loss in fracture toughness at the higher silicon levels. However, microstructure studies did not connect this loss with the appearance of silicides and its cause is presently unknown.

The above data are considered to support a specification maximum of 0.14 percent Si to avoid silicide embrittlement during fan cooling from the solution temperature for section sizes producing through hardening.

Some earlier work (Ref. 22) on conventionally processed Ti-6Al-2Sn-2Zr-1Mo-0.12O (see Table 1.9.1.4) showed similar effects of silicon on the tensile strength and fracture toughness but found no effect of silicon on the fatigue crack propagation rates.

1.9.1.1 *[Table]* Influence of silicon content on the tensile properties and fracture toughness of laboratory heats containing somewhat different equivalent oxygen contents.

1.9.1.2 *[Table]* Influence of silicon content on the tensile properties and fracture toughness of laboratory heats containing somewhat different equivalent oxygen contents and given an intermediate 1500F solution treatment.

1.9.1.3 *[Table]* Influence of silicon content on the tensile properties and fracture toughness of laboratory heats containing somewhat different oxygen equivalents and aged at 1150F.

1.9.1.4 *[Table]* Effect of silicon content on tensile properties and fracture toughness of a Ti-6Al-2Sn-2Zr-1Mo-0.12O alloy.

1.9.2 Solution temperatures in the range of 1500 to 1600F appears to produce a minimum in the tensile yield strength of sheet (see Figures 3.2.1.5 through 3.2.1.7).

1.9.3 Cooling rate from the solution temperature is critical for plate and forgings. Slow rates lead to reduced tensile strengths while very fast rates will increase tensile strength at the expense of reduced fracture toughness. Present recommendations follow the schedule given in Table 1.5.1.3 which specifies fan air cooling. Considering the possible variation in fan size and locations in respect to the part it would be wise to use thermocoupled test pieces to determine the actual cooling rate for a particular part shape and size.

1.9.4 Welding. Attempts to produce satisfactory welds for critical applications have been unsuccessful (see Section 4.3).

2. Physical Properties and Environmental Effects

2.1 Thermal Properties

2.1.1 Melting Range.

2.1.2 Phase Changes.

Beta transus – 1735 to 1785F, dependent upon composition variations given in Table 1.4.1.

2.1.2.1 Time-temperature-transformation diagrams.

2.1.3 Thermal Conductivity.
4 Btu ft per (hr ft^2 F) at room temperature (Ref. 16).

2.1.4 Thermal Expansion.
5.1×10^{-6} in./in./F.

2.1.5 Specific Heat.

2.1.6 Thermal Diffusivity.

2.2 Other Physical Properties

2.2.1 Density.
0.156 lb/cu in. (Refs. 6, 16).

2.2.2 Electrical Properties.

2.2.4 Emittance.

2.2.5 Damping Capacity.

2.3 Chemical Environments

2.3.1 General Corrosion.

2.3.2 Stress Corrosion.

The only data available at the time this Chapter was prepared related to the determination of the effects of stress intensity level on failure time in NaCl solutions. There are presently no published standards for these types of tests and therefore comparision with similar data should be approached with caution.

2.3.2.1 *[Figure]* Effect of applied K level on the failure time of conventionally processed billet in 3.5 percent NaCl.

A quantity designated as K_{Iscc} was recently reported (Ref. 26) for a variety of product forms from four producers. These forms included plates, forgings and forged block (up to 13-inch round corner block) from ingots having 0.23 percent silicon. Bolt-loaded compact specimens [MCT(W)] were cut from these forms and subjected to continuous immersion in 3.5 percent NaCl solution for 1000 hours. The procedures used in these tests have been described in a proposal for an ASTM test method (Ref. 25). While the K value based on the applied load and final crack length is designated as K_{Iscc} there is no assurance that further exposure to the NaCl solution would not have produced a lower value. The results of 35 tests gave an average value of 47.3 ksi $\sqrt{in.}$ with a standard deviation of 4.16. Additional tests on plate material with a 0.15 percent silicon content did not produce significantly different values from material containing 0.23 percent silicon (Ref. 27).

2.4 Nuclear Environments

3. Mechanical Properties

3.1 Specified Mechanical Properties

3.1.1 *[Table]* Producers typical mechanical properties for beta forged plate and billet.

3.2 Mechanical Properties at Room Temperature

3.2.1 Tensile Stress-strain Diagrams and Tensile Properties.

3.2.1.1 Tensile stress-strain diagrams (see Section 3.3.1).

3.2.1.2 *[Table]* Spread of tensile and yield strengths for α-β finished forgings and plates from several producers and different heats.

3.2.1.3 *[Figure]* Effect of oxygen content on the tensile properties of pancake forgings.

3.2.1.4 *[Figure]* Effect of thickness on the transverse tensile properties of conventionally processed sheet and plate.

3.2.1.5 *[Figure]* Effect of solution temperature on tensile properties of mill annealed unaged sheet.

3.2.1.6 *[Figure]* Effect of solution temperature on the transverse tensile properties of unaged sheet and plate.

3.2.1.7 *[Figure]* Effect of solution temperature on the tensile properties of sheet.

3.2.1.8 *[Figure]* Effect of aging temperature on tensile properties of sheet solution treated at 1600F.

3.2.1.9 *[Figure]* Effect of aging temperature on the tensile properties of sheet solution treated at 1700F.

3.2.1.10 *[Figure]* Effect of aging temperature on the tensile yield strength of sheet solution treated at several temperatures.

3.2.1.11 *[Figure]* Effect of 100-hour exposure temperature on the tensile properties of mill annealed sheet.

3.2.2 Compression Stress-strain Diagrams and Compressions Properties.

3.2.2.1 Compression stress-strain diagrams (see Section 3.3.2).

3.2.2.2 *[Table]* Spread of compressive yield strengths for α-β finished forgings and plates from several producers and different heats.

3.2.3 Impact.

3.2.3.1 *[Table]* Impact energy of a conventionally processed plate and a billet given a duplex anneal heat treatment.

3.2.4 Bending. Mill annealed material L and T limit: 3 x thickness at 105 degrees.

3.2.5 Torsion and Shear.

3.2.5.1 *[Table]* Spread of shear ultimate strengths for α-β finished forgings and plates from several producers and different heats.

3.2.5.2 *[Table]* Shear strength of a conventionally processed plate and a forged billet given a duplex anneal heat treatment.

3.2.6 Bearing.

3.2.6.1 *[Table]* Spread of bearing ultimate and yield strengths for α-β finished forgings and plates from several producers and different heats.

3.2.7 Stress Concentration.

3.2.7.1 Notch properties.

3.2.7.2 Fracture toughness. (See Tables 1.3.1, 1.5.1.1, and 1.5.1.2.)

3.2.7.2.1 *[Figure]* Effect of oxygen content on the fracture toughness of pancake forgings.

3.2.7.2.2 *[Figure]* Effect of aging temperature on plane strain fracture toughness of hot rolled plate given a triplex heat treatment.

3.2.8 Combined Loading.

3.3 Mechanical Properties at Various Temperatures

3.3.1 Tension Stress-strain Diagrams and Tensile Properties.

3.3.1.1 *[Figure]* Effect of temperature on longitudinal tensile stress-strain curves for conventionally processed plate.

3.3.1.2 *[Figure]* Effect of temperature on the transverse tensile stress-strain curves for conventionally processed plate.

3.3.1.3 *[Figure]* Effect of temperature on the longitudinal tensile stress-strain curves for α-β finished forged and duplex annealed billet.

3.3.1.4 *[Figure]* Effect of temperature on the transverse tensile stress-strain curves for α-β finished forged and duplex annealed billet.

3.3.1.5 *[Figure]* Effect of elevated temperature on tensile properties of specimens cut from a conventionally processed large billet.

3.3.1.6 *[Figure]* Effect of temperature on the tensile properties of conventionally processed plate.

3.3.1.7 *[Figure]* Effect of temperature on the tensile yield strength of a forging after 100-hour exposure at the test temperature.

3.3.1.8 *[Figure]* Effect of temperature on tensile strength of large forgings from three heats representing two producers (bars and/or points indicate 95 percent confidence intervals).

3.3.1.9 *[Figure]* Effect of temperature and elevated temperature exposure on tensile strength of a large wing strut die forging from one producer (bars indicate one sigma deviation from means).

3.3.2 Compression Stress-strain Diagrams and Compression Properties.

3.3.2.1 *[Figure]* Effect of temperature on the longitudinal compression stress-stain curves for conventionally processed plate.

3.3.2.2 *[Figure]* Effect of temperature on the transverse compression stress-strain curves for conventionally processed plate.

3.3.2.3 *[Figure]* Effect of temperature on the longitudinal compression stress-strain curves for duplex annealed billet.

3.3.2.4 *[Figure]* Effect of temperature on the transverse compression stress-strain curves for duplex annealed billet.

3.3.2.5 *[Figure]* Effect of temperature on the compression yield strength of conventionally processed plate.

3.3.3 Impact.

3.3.4 Bending.

3.3.5 Torsion and Shear.

3.3.6 Bearing.

3.3.7 Stress Concentration.

3.3.7 Notch Properties.

3.3.7.1 Fracture toughness.

3.3.8 Combined Loading.

3.4 Creep and Creep Rupture Properties

3.4.1 *[Figure]* Plastic creep and rupture data for conventionally processed plate and duplex annealed billet.

3.5 Fatigue Properties

3.5.1 Conventional High-cycle Fatigue.

3.5.1.1 *[Figure]* Effect of test temperature on the smooth fatigue strength of conventionally processed billet.

3.5.1.2 *[Figure]* Effect of test temperature on the notched fatigue strength of conventionally processed plate.

3.5.1.3 *[Figure]* Effect of test temperature on smooth fatigue strength of conventionally processed plate.

3.5.1.4 *[Figure]* Notch fatigue strength for conventionally processed solution treated unaged plate.

3.5.1.5 *[Figure]* Notch fatigue strength for conventionally processed plate.

3.5.1.6 *[Figure]* Notch fatigue strength of a conventionally processed forging.

3.5.1.7 *[Figure]* Smooth fatigue strength produced by two thermomechanical processes applied to Ti-6-2-2-2-2 forgings compared with fatigue strength of annealed Ti-6Al-4V forgings.

3.5.1.8 *[Figure]* Notch fatigue strength produced by two thermomechanical processes applied to Ti-6-2-2-2-2 forgings compared with fatigue strength of annealed Ti-6Al-4V forgings.

3.5.2 Low-cycle Fatigue.

3.5.2.1 *[Figure]* Effect of thermomechanical processing on low cycle fatigue crack initiation of forgings.

3.5.3 Fatigue Crack Propagation.

3.5.3.1 *[Figure]* Fatigue crack growth rates at 1 Hz for conventionally processed plate in humid air and in 3.5 percent NaCl.

3.5.3.2 *[Figure]* Fatigue crack growth rates at 20 Hz for conventionally processed plate in humid air and in 3.5 percent NaCl.

3.5.3.3 *[Figure]* Fatigue crack growth rates at 1 Hz for conventionally processed solution treated unaged plate in humid air and in 3.5 percent NaCl.

3.5.3.4 *[Figure]* Fatigue crack growth rates at 20 Hz for conventionally processed solution treated unaged plate in humid air and in 3.5 percent NaCl.

3.5.3.5 *[Figure]* Fatigue crack growth rates for conventionally processed forging in dry air and in 3.5 percent NaCl.

3.5.3.6 *[Figure]* Fatigue crack growth rates for Ti-6-2-2-2-2 forgings subjected to several thermomechanical processes compared with beta mill annealed Ti-6Al-4V forgings.

3.5.3.7 *[Figure]* Fatigue crack growth rates in 3.5 percent NaCl for hand forgings made from 8000-lb ingot and subjected to several thermomechanical processes.

3.5.3.8 *[Figure]* Fatigue crack growth rates for forgings subjected to several thermomechanical processes.

3.6 Elastic Properties

3.6.1 Poisson's Ratio.

3.6.2 Modulus of Elasticity.
For α-β finish forge + triplex heat treat = 17,200 ksi; for β finish forge + triplex heat treat = 16,000 ksi (Ref. 6).

3.6.2.1 *[Figure]* Effect of temperature on the tension and compression elastic modulus of conventionally processed plate.

3.6.2.2 *[Figure]* Effect of temperature on the tension and compression elastic modulus of conventionally processed forged billet.

3.6.3 Modulus of Rigidity.

3.6.4 Tangent Modulus.

3.6.5 Secant Modulus.

4. Fabrication

4.1 Forming

4.1.1 Superplastic Forming. Recent studies have shown that sheet can be superplastically formed using the same procedures as employed for Ti-6Al-4V and with no greater difficulties (Ref. 19).

4.1.2 *[Figure]* Effect of superplastic forming temperature on the tensile properties of sheet.

4.2 Machining and Grinding

4.3 Joining

4.3.1 Welding. There has been very little information published on the weldability of this alloy. Recent aircraft applications have not involved welding. Attempts to electron beam weld plate were reported as unsuccessful (Ref. 23). Weld tensile properties were essentially equal to the parent metal but the fracture toughness of the welds was low as evidenced by specimens fracturing during fatigue cracking. At the time of this Chapter preparation welding can not be recommended.

4.3.1.1 *[Table]* Tensile properties and fracture toughness of electron beam welds in conventionally processed plate.

4.4 Surface Treating

Table 1.3.1 Proposed design mechanical property values for α-β processed forgings and plate (Ref. 16)

Alloy	Ti-6-2-2-2-2			
Condition	Triplex Heat Treatment (see Table 1.5.1.3)			
Form	Die Forgings		Forged Block	Plate
Direction	**L, LT & ST**			**L & LT**
Size (in.)	**≤ 3-in.**		**13-in.[a]**	**≤ 3-in.**
Basis	**S**	**B**	**S**	
F_{tu} (ksi)	150[b]	156	150	150
F_{ty} (ksi)	135	138	135	135
F_{cy} (ksi)	146	150	146	146
F_{su} (ksi)	96	100	96	96
F_{bru} (ksi)				
e/D = 1.5	239	248	239	239
e/D = 2	297	309	237	237
F_{bry} (ksi)				
e/D = 1.5	217	222	217	217
e/D = 2	260	266	260	260
e (percent)	5	–	5	5
K_{Ic} (ksi $\sqrt{in.}$)	70	–	70	70
E (1000 ksi)	17.2	17.2	17.2	17.2
G (1000 ksi)	6.5	6.5	6.5	6.5
μ	0.33	0.33	0.33	0.33

[a] Heat treated size ≤ 3 inches.

[b] F_{tu} A value = 152 ksi.

Table 1.4.1 Chemical composition (Refs. 1, 28)

Alloy	Ti-6-2-2-2-2			
Composition	Conventional (Ref. 1)		Modified for Higher Toughness (Ref. 28)	
Element	**Min**	**Max**	**Min**	**Max**
Al	5.25	6.25	5.25	6.25
Sn	1.75	2.25	1.75	2.25
Zr	1.75	2.25	1.75	2.25
Mo	1.75	2.25	1.75	2.25
Cr	1.75	2.25	1.75	2.25
Si	0.20	0.27	0.12	0.20
C	–	0.04	–	0.04
N	–	0.03	–	0.03
Fe	–	0.25	–	0.15
O_2	–	0.14	–	0.13
H_2[a]	–	–	–	125 ppm

[a] Determined on finished parts.

Table 1.5.1.1 Effect of thermal mechanical processing on the tensile properties and fracture toughness of pancake forgings (Refs. 4, 7)

Alloy		Ti-6-2-2-2-2						
Composition		6Al - 2.2Sn - 1.8Zr - 2.1Cr - 1.9Mo - 0.16Si - 0.076O$_2$ - 0.01N - 0.02C - 0.06Fe						
Form		6-in. dia x 1.7-in. Thick Pancake Forgings						
Specimen Orientation		Tangential						
Process Forge	**Preform Forge**	**Finish Forge**[a]	**Heat / Heat Treatment**[b]	**F_{tu} (ksi)**	**F_{ty} (ksi)**	**e (percent)**	**RA (percent)**	**K_{Ic} (ksi $\sqrt{in.}$)**
1	α-β	β_t + 82F	β_t - 72F, 1 hr, FAC + 1000F, 8 hr, AC	161	144	11	21	82
2		β_t + 122F		162	145	12	21	80
3	β	α - β 25 percent		163	150	12	23	62
4		α - β 50 percent		162	149	12	25	53
5	α-β	α - β 50 percent	β_t + 82F, 0.5 hr, FAC + 1000F, 8 hr, AC	161	139	10	15	68
6		α - β 50 percent	β_t + 82F, 0.5 hr, FAC β_t - 122F, 1 hr, AC + 1000F, 8 hr, AC	159	141	10	17	77

a β_t = β transus temperature. Percentages = forge reduction.

b β_t = β transus temperature. FAC = fan air cool.

Table 1.5.1.2 Effect of several thermal mechanical processes on the tensile properties and fracture toughness of forgings (Refs. 6, 7)

Alloy	Ti-6-2-2-2-2								
Form	Forgings								
Forging Type	**Forge Process**[a]	**Heat Treatment**	**Section Thickness (in.)**	**Direction**	**F_{tu} (ksi)**	**F_{ty} (ksi)**	**e (percent)**	**RA (percent)**	**K_{Ic} (ksi $\sqrt{in.}$)**
Pancake 0.076 Oxygen	$> \beta_t$	α-β[b] FAC[c]	0.5	L T	163 157	146 142	10 9	17 15	74 TL
	α-β	Triplex[d] FAC	0.5	L T	159 155	141 137	10 9	16 15	78 TL
Pancake 0.13 Oxygen	$> \beta_t$	α-β FAC	–	L T	154 152	138 137	12 13	17 18	79 TL
	α-β	Triplex Oil Quench	1.5	L T	176 169	154 152	8 7	12 11	63 TL
Closed Die 0.13 Oxygen	$> \beta_t$	α-β FAC	3 1 1 0.5	L L T T	163 161 160 165	146 144 148 147	12 11 13 17	21 19 24 26	71 SL
	α-β	Triplex FAC	3 1 1 0.05	L L T T	154 159 154 159	138 141 137 144	10 19 9 14	17 24 16 18	74 SL

[a] $> \beta_t$ = finish forge above the β transus. α - β = through transus forge.

[b] ST β_t - 75F, 0.5 hour, FAC + 1000F, 8 hours, AC (conventional heat treat).

[c] FAC = fan air cool > 35 degrees per minute.

[d] ST β_t + 82F, 0.5 hour, FAC + β_t - 122F, 1 hour, AC + 1000F, 8 hours, AC.

Table 1.5.1.3 Triplex heat treatments specified for α-β finished forgings and plate (Ref. 16)

Alloy	Ti-6-2-2-2-2	
Form	Forgings and Plate (with maximum thickness or diameter up to 3-in.)	
β Solution Heat Treatment	**α - β Solution Treatment following β Solution Treatment**	**Aging**
Range: β transus[a] + 25F to β transus + 100F, 0.5 hr min, Fan Air Cool 36 to 120F/min to 900F max	Range: β transus - 25F to β transus - 115F, 1 hr min, Fan Air Cool 36 to 120F/min	925 to 1025F 8 to 10 hr, AC

[a] β transus to be determined to within +/- 25F.

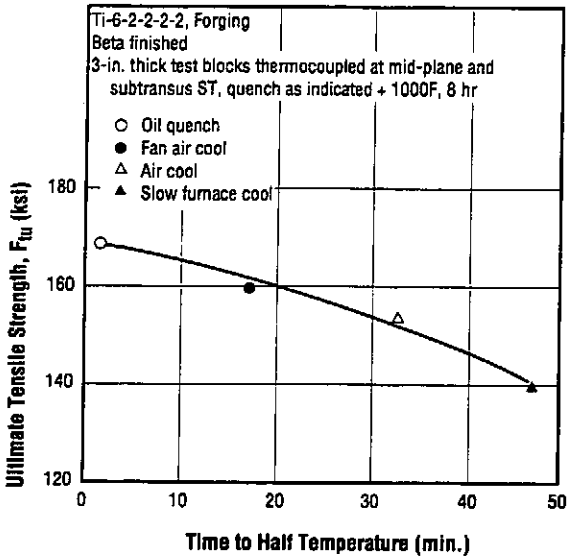

Fig. 1.5.1.4 Effect of cooling rate on the tensile strength of a forging (Ref. 20)

Table 1.9.1.1 Influence of silicon content on the tensile properties and fracture toughness of laboratory heats containing somewhat different equivalent oxygen contents (Ref. 24)

Alloy	Ti-6-2-2-2-2			
Form	65-lb Ingots Converted to 1.75-in. Thick Plate			
Heat Treatment	Triplex (see Table 1.5.1.3)			
Composition	**0.03 Si 0.18 Oe**[a]	**0.14 Si 0.13 Oe**	**0.24 Si 0.16 Oe**	**0.30 Si 0.18 Oe**
F_{tu} (ksi)[b]	163	164	174	176
F_{ty} (ksi)	145	143	152	155
e (percent)	8	9	9	8
RA (percent)	16	15	14	14
K_{Ic} (ksi $\sqrt{in.}$)[c]	79	88	73	63

[a] Oe = Oxygen equivalent = percent Oxygen + 1.5 percent Nitrogen.

[b] Average L and T.

[c] LT C(T) specimens.

Table 1.9.1.2 Influence of silicon content on the tensile properties and fracture toughness of laboratory heats containing somewhat different equivalent oxygen contents and given an intermediate 1500F solution treatment (Ref. 24)

Alloy	Ti-6-2-2-2-2			
Form	65-lb Ingots Converted to 1.75-in. Thick Plate			
Heat Treatment	β + 50F 1 hr, FAC[a] + β - 50F 1 hr, FAC + 1500F 2 hr, FAC + 1000F 8 hr, AC			
β Transus (F)	1805	1785	1810	1820
Composition	**0.03 Si 0.18 Oe**[b]	**0.14 Si 0.13 Oe**	**0.24 Si 0.16 Oe**	**0.30 Si 0.18 Oe**
F_{tu} (ksi)[c]	162	161	166	169
F_{ty} (ksi)	144	141	148	152
e (percent)	8	6	4	7
RA (percent)	15	8	7	13
K_{Ic} (ksi $\sqrt{in.}$)[d]	62	61	48	46

a FAC = fan air cool.

b Oe = Oxygen equivalent = percent Oxygen + 1.5 percent Nitrogen.

c Average L and LT.

d LT C(T) specimens.

Table 1.9.1.3 Influence of silicon content on the tensile properties and fracture toughness of laboratory heats containing somewhat different oxygen equivalents and aged at 1150F (Ref. 24)

Alloy	Ti-6-2-2-2-2			
Form	65-lb Ingots Converted to 1.75-in. Thick Plate			
Heat Treatment	β + 50F 1 hr, FAC[a] + β - 50F 1 hr, FAC + 1150F 8 hr, AC			
β Transus (F)	1895	1785	1810	1820
Composition	**0.03 Si 0.18 Oe**[b]	**0.14 Si 0.13 Oe**	**0.24 Si 0.16 Oe**	**0.30 Si 0.18 Oe**
F_{tu} (ksi)[c]	156	157	166	168
F_{ty} (ksi)	145	146	155	157
e (percent)	13	8	8	7
RA (percent)	19	12	10	9
K_{Ic} (ksi $\sqrt{in.}$)[d]	78	68	49	43

a FAC = fan air cool.
b Oe = Oxygen equivalent = percent Oxygen + 1.5 percent Nitrogen.
c Average L and LT.
d LT C(T) specimens.

Table 1.9.1.4 Effect of silicon content on tensile properties and fracture toughness of a Ti-6Al-2Sn-2Zr-1Mo-0.12O alloy (Ref. 22)

Alloy	Ti-6Al-2Sn-2Zr-1Mo-0.12O + Si					
Form	1.26 x 5-in. Sheet Bar Rolled at 1950F					
Condition	ST 1950F, 15 min., AC + 1300F, 2 hr, AC					
Silicon (percent)	**0**		**0.25**		**0.5**	
Test Temperature (F)	**77**	**1000**	**77**	**1000**	**77**	**1000**
F_{tu} (ksi)	127	78	141	86	143	94
F_{ty} (ksi)	107	654	119	66	119	71
e (percent)	7.8	11.9	7	10	3.5	7
K_Q (ksi $\sqrt{in.}$)	112	103	86[a]	89	71[a]	87

a K_{Ic} values.

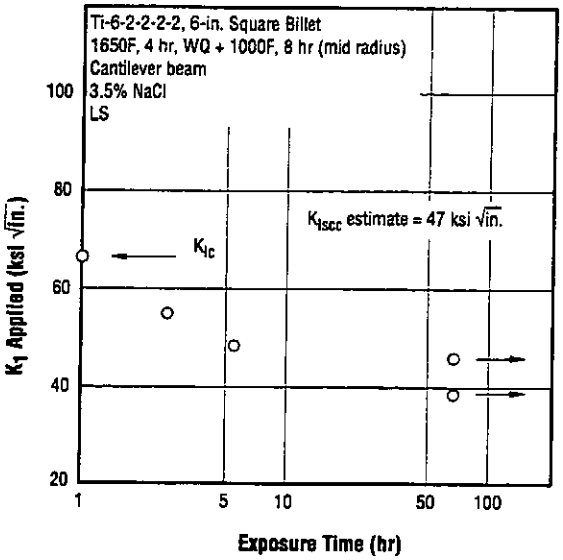

Fig. 2.3.2.1 Effect of applied K level on the failure time of conventionally processed billet in 3.5 percent NaCl (Ref. 3)

Table 3.1.1 Producers typical mechanical properties for beta forged plate and billet (Ref. 1)

Alloy	Ti-6-2-2-2-2		
Condition	Beta Forged + Subtransus ST + 1000F Age		
Form	**2-in. Plate**	**4-in. Plate**	**6-in. Rectangular Billet**
F_{tu} (ksi)	168	160	164
F_{ty} (ksi)	148	142	147
e (percent)	10	10	9
RA (percent)	16	14	13
K_{Ic} (ksi √in.)	77	81	89

Table 3.2.1.2 Spread of tensile and yield strengths for α-β finished forgings and plates from several producers and different heats (Ref. 16)

Alloy		Ti-6-2-2-2-2																				
Producer		Wyman Gordon			ALCOA			RMI		TIMET				RMI						TIMET		
Form[a]		Die Forging						2-in. Plate						6-in. Plate								
No. Lots[b]		**3**						**1**		**2**		**3**		**1**								
Heat		**NS[c]**			**NS**			**882794**		**G6591**				**873190**			**882890**			**G6591**		
Direction		**L**	**LT**	**ST**	**L**	**LT**	**ST**	**L**	**LT**	**L**	**LT**	**L**	**LT**	**L**	**LT**	**ST**	**L**	**LT**	**ST**	**L**	**LT**	**ST**
Tests / Lot		**5**	**7**	**7**	**7**	**7**	**7**	**14**	**14**	**14**	**14**	**10**	**10**	**22**	**20**	**20**	**20**	**20**	**20**	**22**	**19**	**20**
F_{tu} (ksi)	max	167	170	168	164	163	160	165	168	167	170	170	174	164	165	163	164	165	164	172	168	166
	min	162	160	161	156	157	153	161	163	161	162	162	165	169	160	159	159	160	169	155	159	157
F_{ty} (ksi)	max	146	146	146	143	143	141	146	147	148	151	148	151	145	145	144	144	145	143	144	147	145
	min	140	138	141	138	137	134	140	143	142	145	142	144	142	140	141	140	140	139	138	138	140

[a] Triplex heat treatment for all forms (see Table 1.5.1.3).

[b] A lot is an individual forging or plate.

[c] NS = not specified.

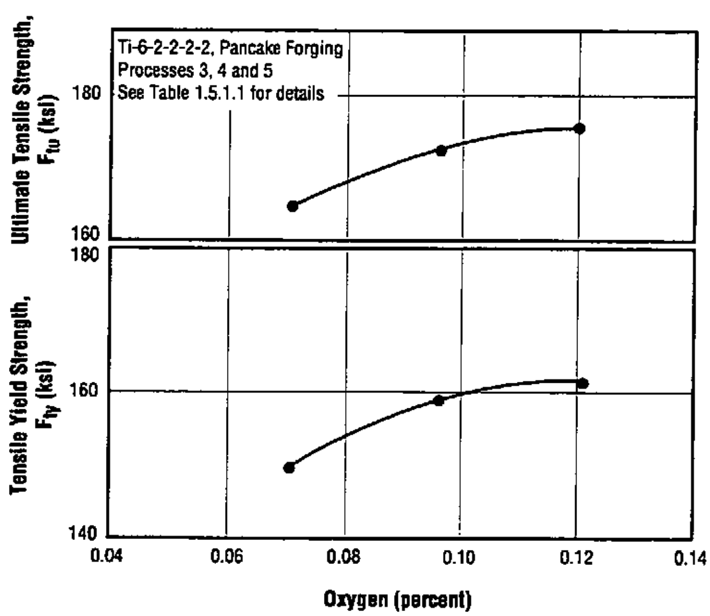

Fig. 3.2.1.3 Effect of oxygen content on the tensile properties of pancake forgings (Ref. 4)

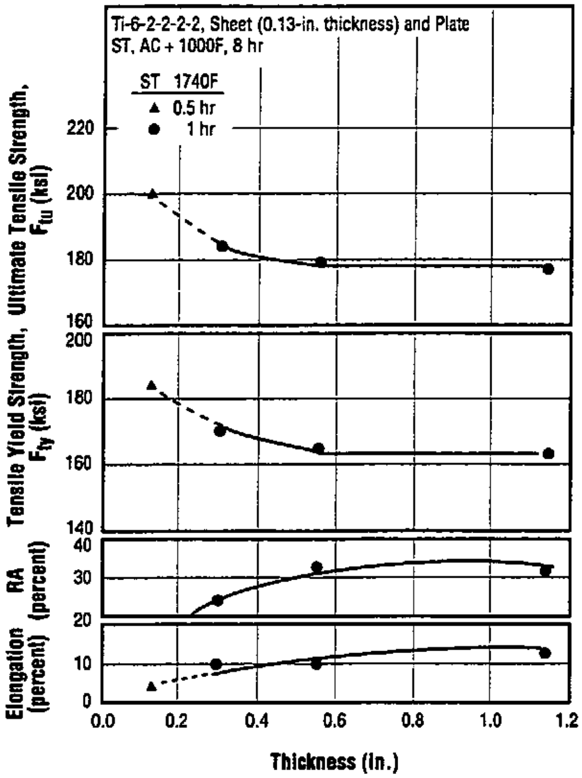

Fig. 3.2.1.4 Effect of thickness on the transverse tensile properties of conventionally processed sheet and plate (Ref. 14)

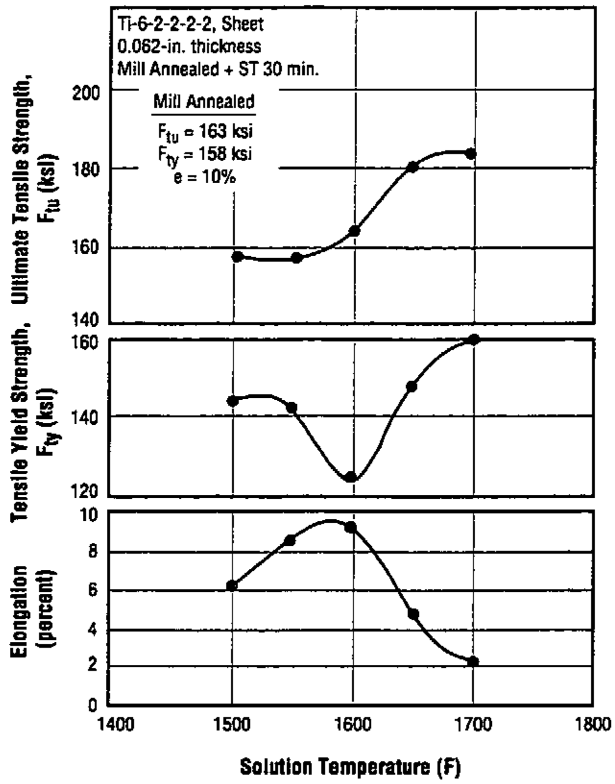

Fig. 3.2.1.5 Effect of solution temperature on tensile properties of mill annealed unaged sheet (Refs. 3, 19)

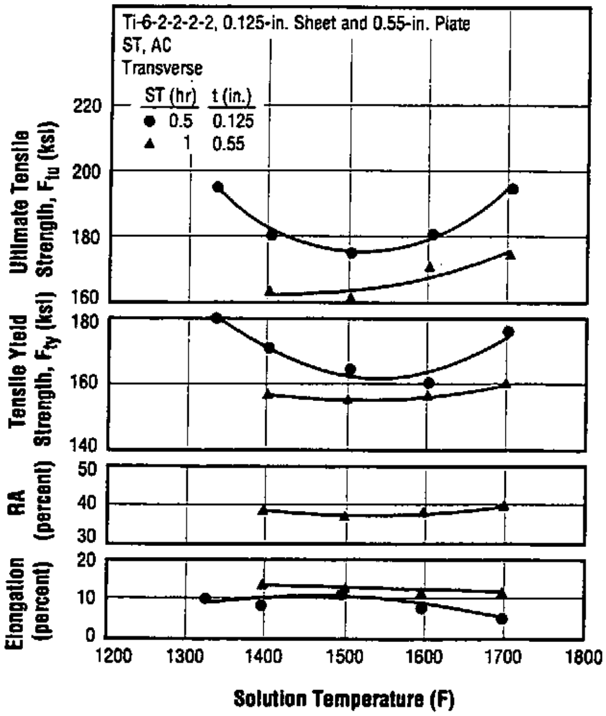

Fig. 3.2.1.6 Effect of solution temperature on the transverse tensile properties of unaged sheet and plate (Ref. 14)

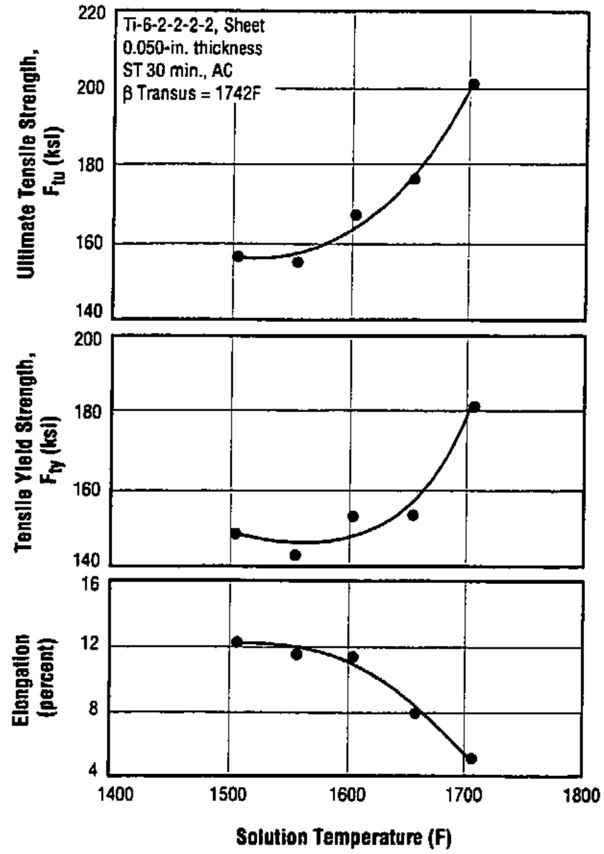

Fig. 3.2.1.7 Effect of solution temperature on the tensile properties of sheet (Ref. 21)

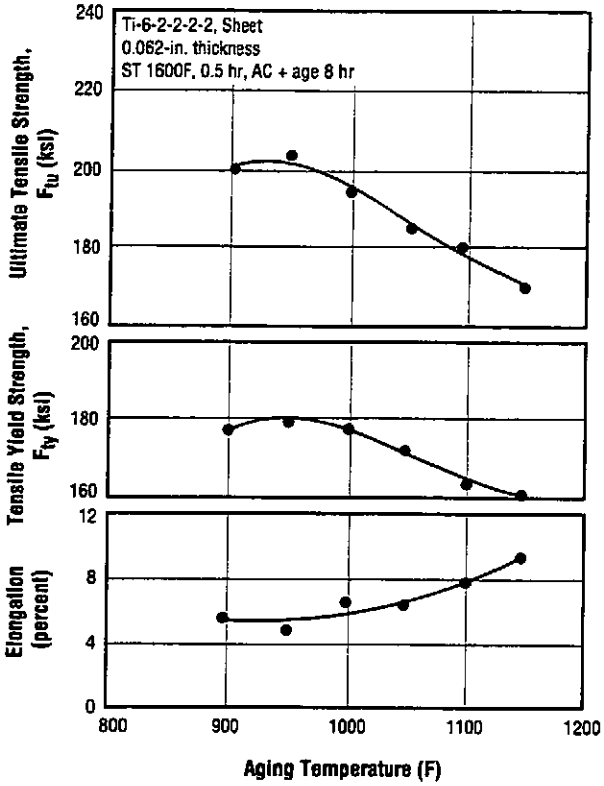

Fig. 3.2.1.8 Effect of aging temperature on tensile properties of sheet solution treated at 1600F (Refs. 3, 19)

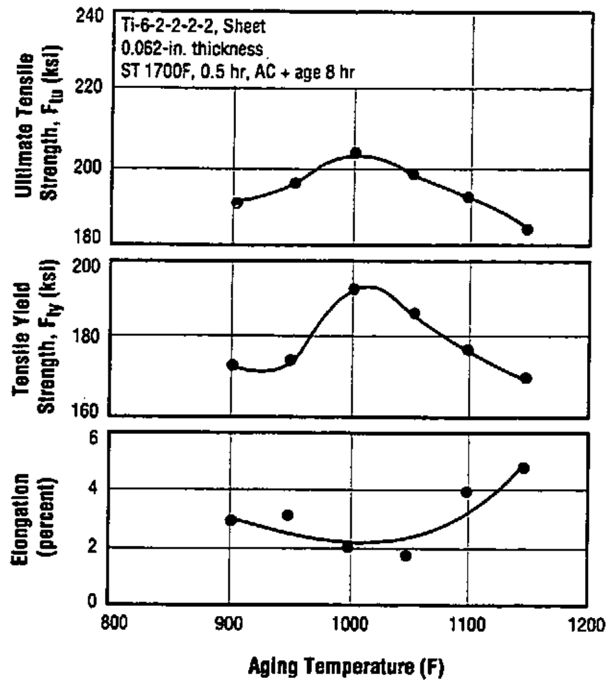

Fig. 3.2.1.9 Effect of aging temperature on the tensile properties of sheet solution treated at 1700F (Refs. 3, 19)

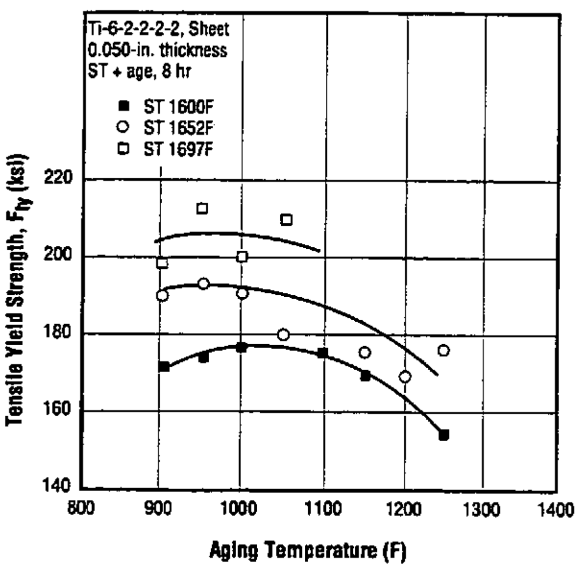

Fig. 3.2.1.10 Effect of aging temperature on the tensile yield strength of sheet solution treated at several temperatures (Ref. 21)

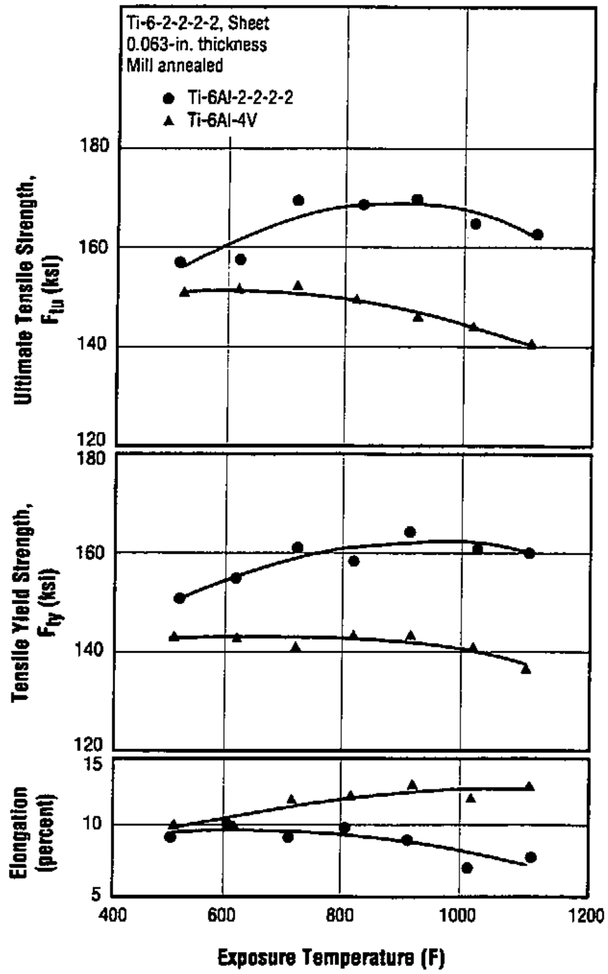

Fig. 3.2.1.11 Effect of 100-hour exposure temperature on the tensile properties of mill annealed sheet (Ref. 19)

Table 3.2.2.2 Spread of compressive yield strengths for α-β finished forgings and plates from several producers and different heats (Ref. 16)

Alloy		Ti-6-2-2-2-2																				
Producer		Wyman Gordon			ALCOA			RMI		TIMET				RMI						TIMET		
Form[a]		Die Forging						2-in. Plate						6-in. Plate								
No. Lots[b]		**3**						**1**		**2**		**3**		**1**								
Heat		**NS[c]**			**NS**			**882794**		**G6591**				**873190**			**882890**			**G6591**		
Direction		**L**	**LT**	**ST**	**L**	**LT**	**ST**	**L**	**LT**	**L**	**LT**	**L**	**LT**	**L**	**LT**	**ST**	**L**	**LT**	**ST**	**L**	**LT**	**ST**
Tests / Lot		**2**	**2**	**2**	**2**	**1**	**1**	**2**	**2**	**3**	**3**	**2**	**2**	**3**	**3**	**3**	**3**	**3**	**3**	**3**	**3**	**3**
F_{cy} (ksi)	max	160	156	160	153	153	152	159	159	169	169	157	160	157	154	156	155	157	157	163	155	158
	min	154	150	155	150	153	150	149	159	161	159	157	159	154	152	153	151	154	154	147	149	153

[a] Triplex heat treatment for all forms (see Table 1.5.1.3).

[b] A lot is an individual forging or plate.

[c] NS = not specified.

Table 3.2.3.1 Impact energy of a conventionally processed plate and a billet given a duplex anneal heat treatment (Refs. 8, 15)

Alloy	Ti-6-2-2-2-2			
Source	Table 32 (Ref. 8)		Table 34 (Ref. 15)	
Form	1-1/2-in. Plate		4 x 6-in. Billet	
Condition	**1740F, 1 hr, AC + 1000F, 8 hr**		**1745F, 1 hr, AC to 1560F, WQ + 1000F, 8 hr**	
Direction	**L**	**T**	**L**	**T**
Impact Energy (ft-lb)	14	16	15	-

Table 3.2.2.2 Spread of compressive yield strengths for α-β finished forgings and plates from several producers and different heats (Ref. 16)

Alloy		Ti-6-2-2-2-2																				
Producer		Wyman Gordon			ALCOA			RMI		TIMET				RMI						TIMET		
Form[a]		Die Forging						2-in. Plate						6-in. Plate								
No. Lots[b]		**3**						**1**		**2**		**3**		**1**								
Heat		**NS[c]**			**NS**			**882794**		**G6591**				**873190**			**882890**			**G6591**		
Direction		**L**	**LT**	**ST**	**L**	**LT**	**ST**	**L**	**LT**	**L**	**LT**	**L**	**LT**	**L**	**LT**	**ST**	**L**	**LT**	**ST**	**L**	**LT**	**ST**
Tests / Lot		**2**	**2**	**2**	**2**	**1**	**1**	**2**	**2**	**3**	**3**	**2**	**2**	**3**	**3**	**3**	**3**	**3**	**3**	**3**	**3**	**3**
F_{cy} (ksi)	max	160	156	160	153	153	152	159	159	169	169	157	160	157	154	156	155	157	157	163	155	158
	min	154	150	155	150	153	150	149	159	161	159	157	159	154	152	153	151	154	154	147	149	153

[a] Triplex heat treatment for all forms (see Table 1.5.1.3).

[b] A lot is an individual forging or plate.

[c] NS = not specified.

Table 3.2.5.2 Shear strength of a conventionally processed plate and a forged billet given a duplex anneal heat treatment (Refs. 8, 15)

Alloy	Ti-6-2-2-2-2			
Source	Table 31 (Ref. 8)		Table 33 (Ref. 15)	
Form	1-1/2-in. Plate		4 x 6-in. Billet	
Condition	**1740F, 1 hr, AC + 1000F, 8 hr**		**1745F, 1 hr, AC to 1560F, WQ + 1000F, 8 hr**	
Direction	**L**	**T**	**L**	**T**
F_{su} (ksi)	108	180	103	105

Table 3.2.6.1 Spread of bearing ultimate and yield strengths for α-β finished forgings and plates from several producers and different heats (Ref. 16)

Alloy		Ti-6-2-2-2-2															
Producer		Wyman Gordon		ALCOA		RMI		TIMET				RMI				TIMET	
Form[a]		Die Forging				2-in. Plate						6-in. Plate					
No. Lots[b]		3				1										2	
Heat		NS[c]		NS		882794		G6591				873190		882890		G6591	
Direction		L								LT		L					
Tests / Lot		2					1	3				2	1	3			
e/D		1.5	2	1.5	2	1.5	2	1.5	2	1.5	2	1.5	2	1.5	2	1.5	2
F_{bu} (ksi)	max	270	334	259	322	277	323	259	331	260	308	270	340	266	345	273	334
	min	259	329	255	313	259	–	253	320	244	307	266	–	260	328	250	319
F_{by} (ksi)	max	241	286	232	275	238	268	243	278	225	260	239	290	237	286	243	288
	min	229	285	226	274	222	–	223	256	214	252	239	–	230	278	220	273

a Triplex heat treatment for all forms (see Table 1.5.1.3).
b A lot is an individual forging or plate.
c NS = not specified.

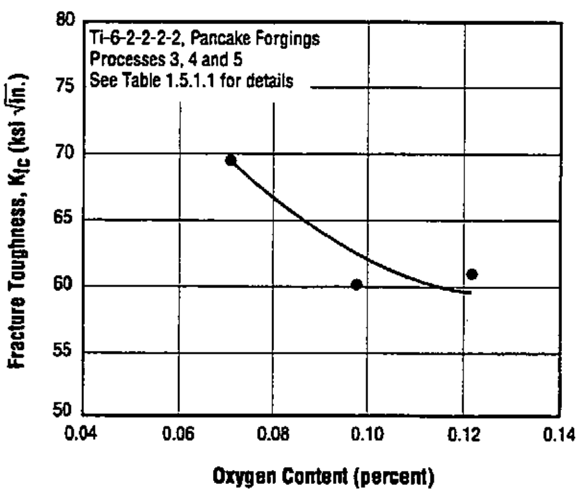

Fig. 3.2.7.2.1 Effect of oxygen content on the fracture toughness of pancake forgings (Ref. 4)

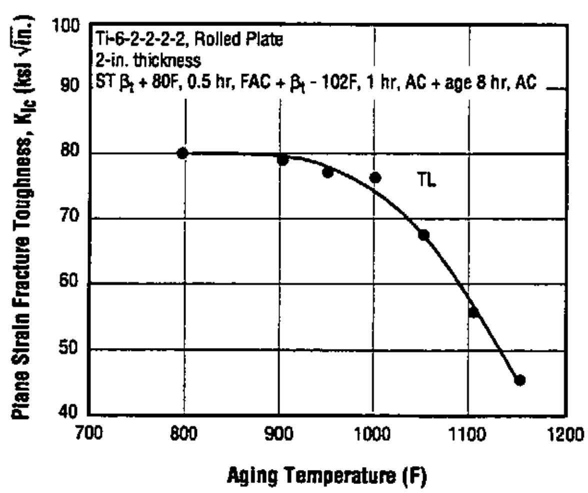

Fig. 3.2.7.2.2 Effect of aging temperature on plane strain fracture toughness of hot rolled plate given a triplex heat treatment (Ref. 5)

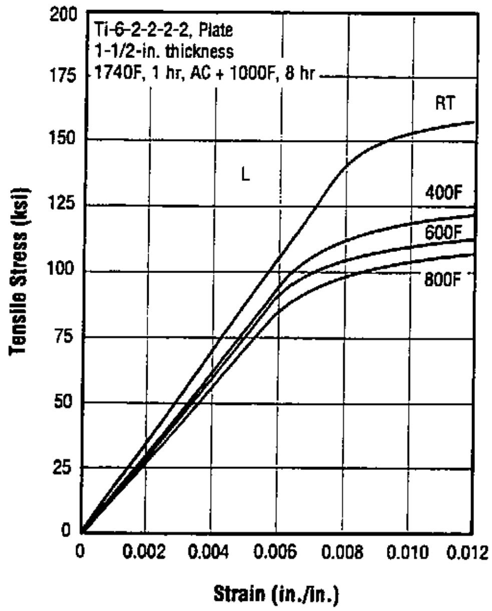

Fig. 3.3.1.1 Effect of temperature on longitudinal tensile stress-strain curves for conventionally processed plate (Ref. 8)

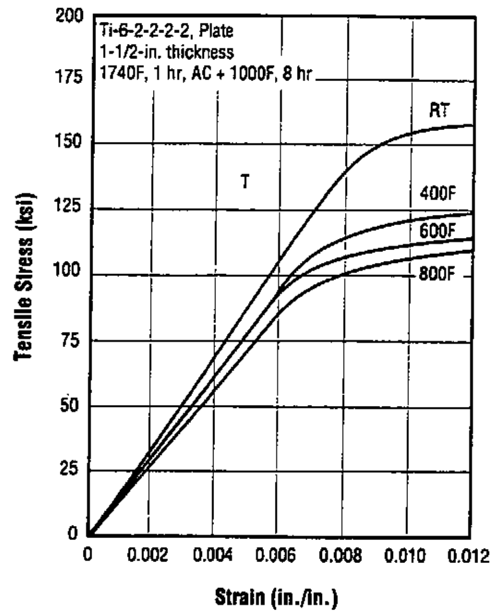

Fig. 3.3.1.2 Effect of temperature on the transverse tensile stress-strain curves for conventionally processed plate (Ref. 8)

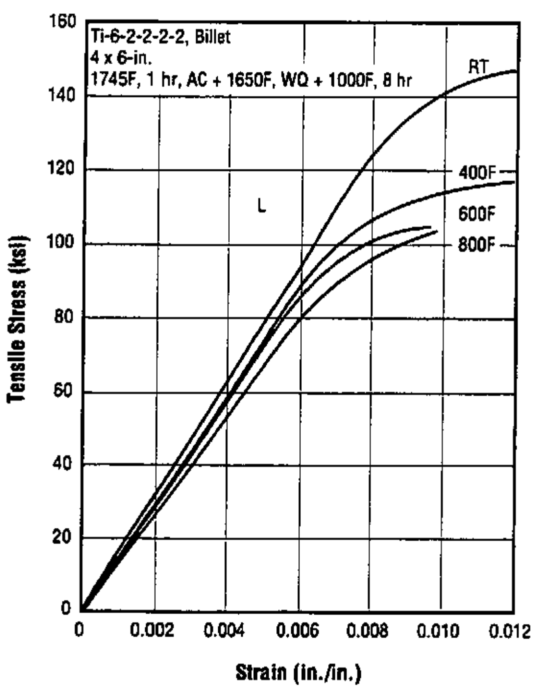

Fig. 3.3.1.3 Effect of temperature on the longitudinal tensile stress-strain curves for α-β finished forged and duplex annealed billet (Ref. 15)

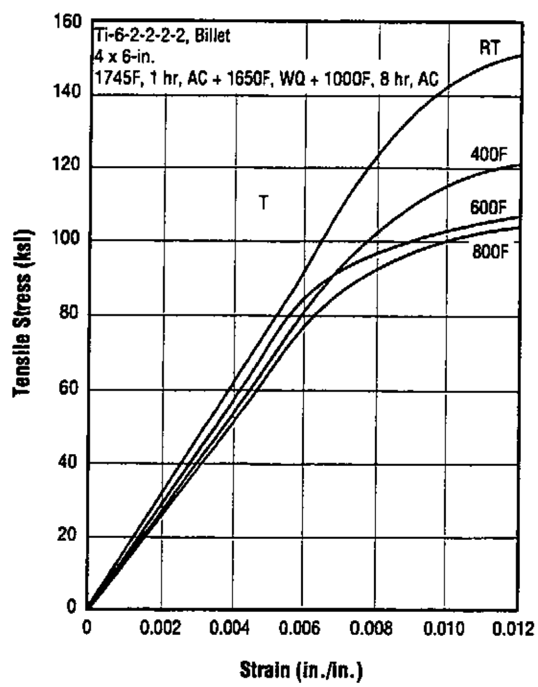

Fig. 3.3.1.4 Effect of temperature on the transverse tensile stress-strain curves for α-β finished forged and duplex annealed billet (Ref. 15)

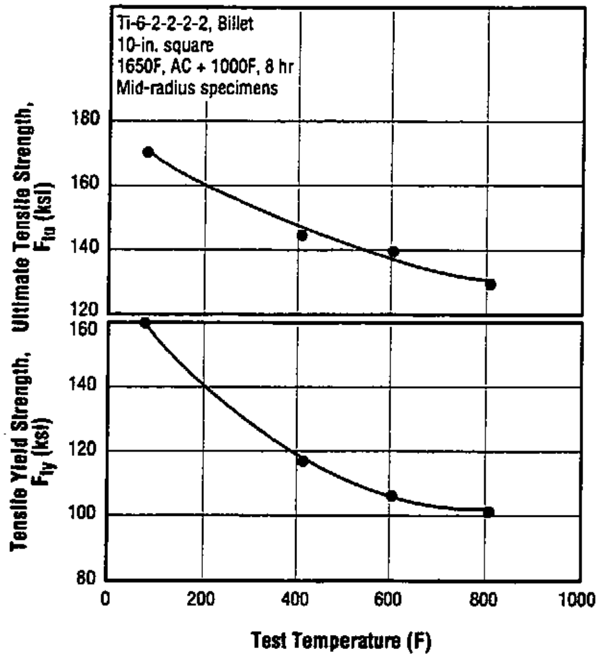

Fig. 3.3.1.5 Effect of elevated temperature on tensile properties of specimens cut from a conventionally processed large billet (Ref. 3)

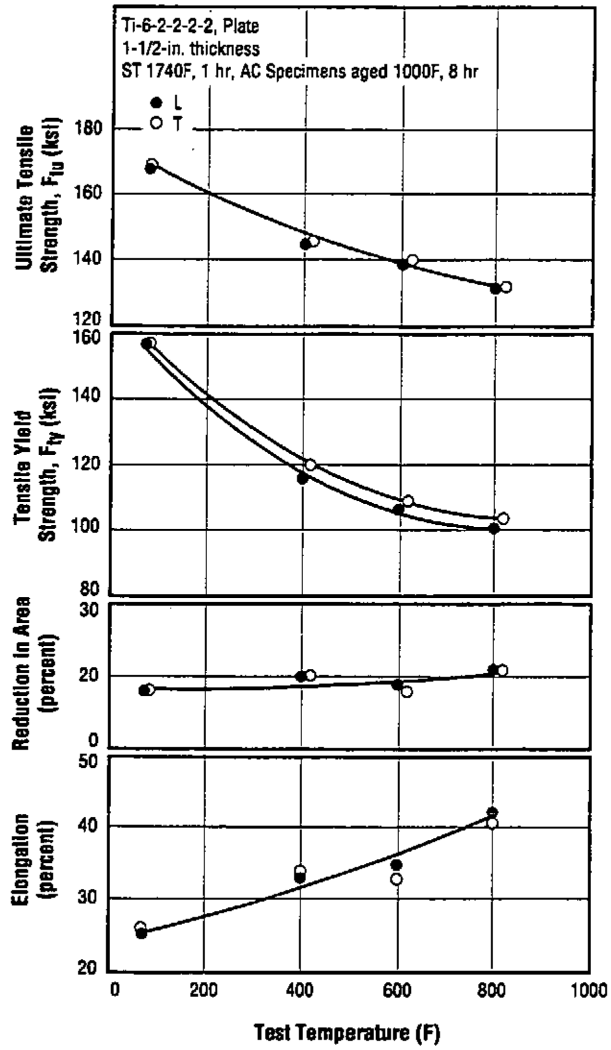

Fig. 3.3.1.6 Effect of temperature on the tensile properties of conventionally processed plate (Ref. 8)

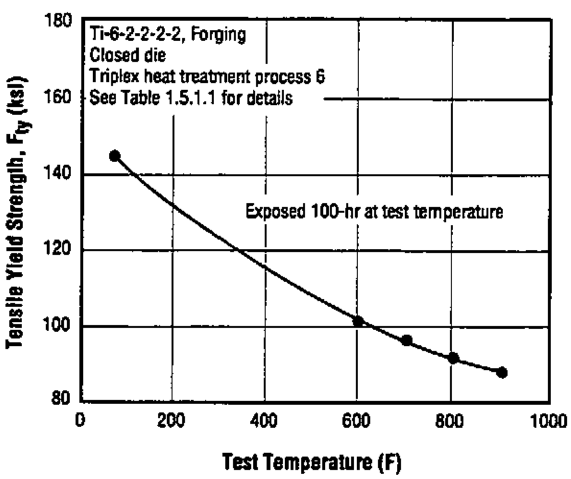

Fig. 3.3.1.7 Effect of temperature on the tensile yield strength of a forging after 100-hour exposure at the test temperature (Ref. 6)

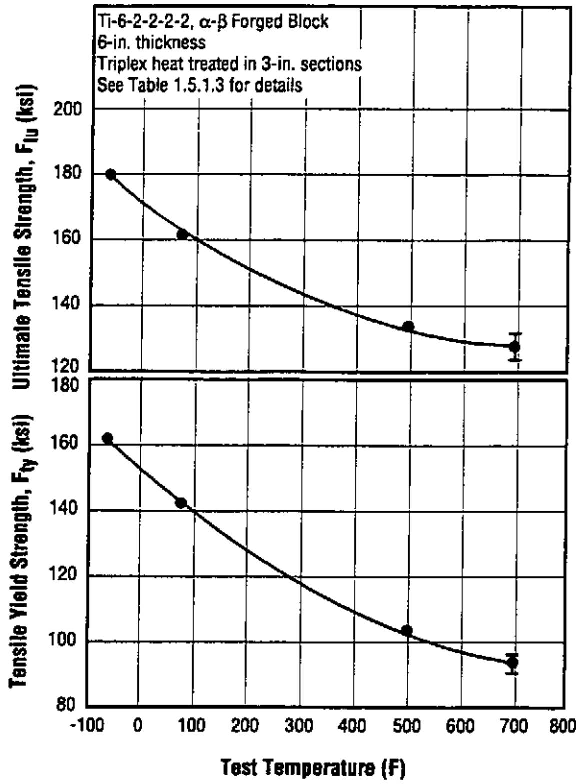

Fig. 3.3.1.8 Effect of temperature on tensile strength of large forgings from three heats representing two producers (bars and/or points indicate 95 percent confidence intervals) (Ref. 16)

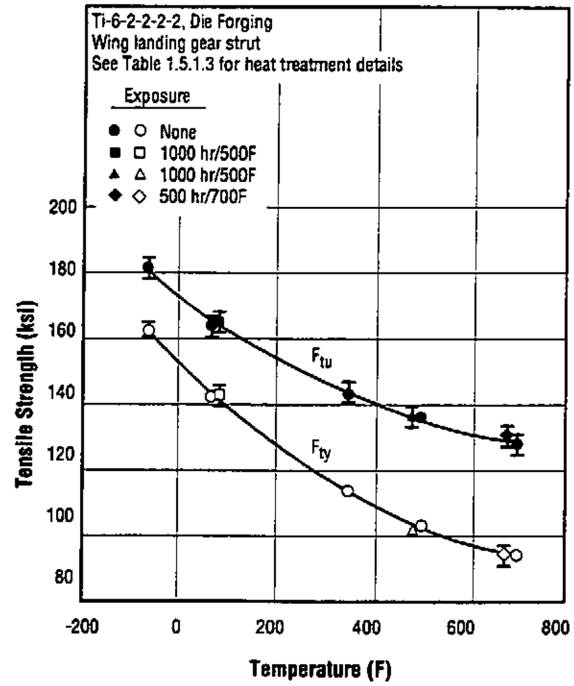

Fig. 3.3.1.9 Effect of temperature and elevated temperature exposure on tensile strength of a large wing strut die forging from one producer (bars indicate one sigma deviation from means) (Ref. 16)

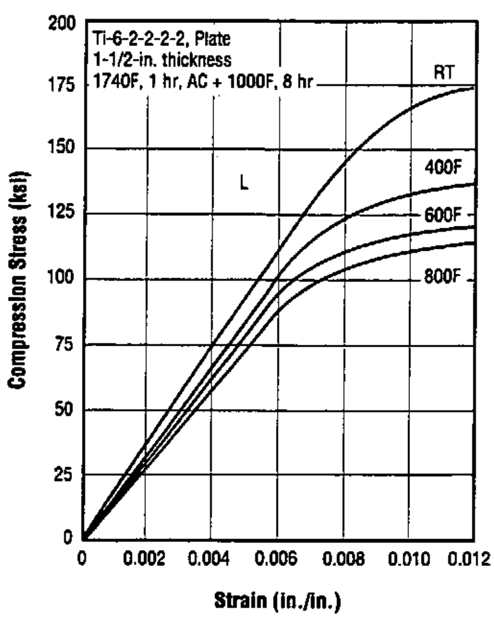

Fig. 3.3.2.1 Effect of temperature on the longitudinal compression stress-strain curves for conventionally processed plate (Ref. 8)

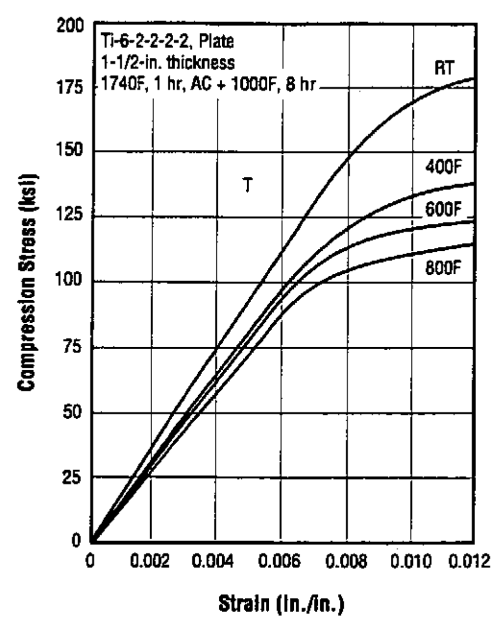

Fig. 3.3.2.2 Effect of temperature on the transverse compression stress-strain curves for conventionally processed plate (Refs. 8, 15)

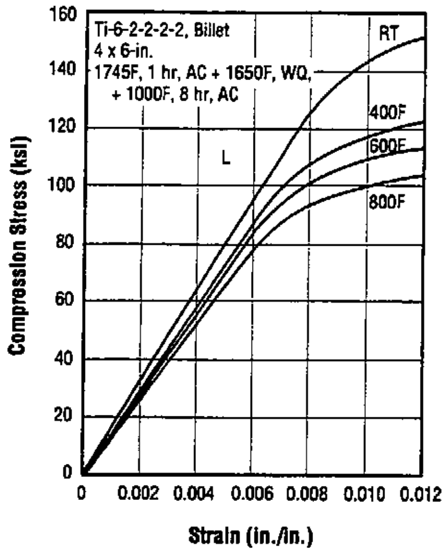

Fig. 3.3.2.3 Effect of temperature on the longitudinal compression stress-strain curves for duplex annealed billet (Ref. 15)

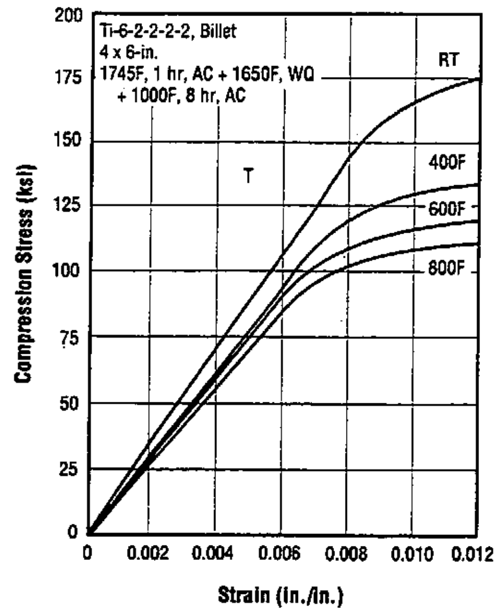

Fig. 3.3.2.4 Effect of temperature on the transverse compression stress-strain curves for duplex annealed billet (Ref. 15)

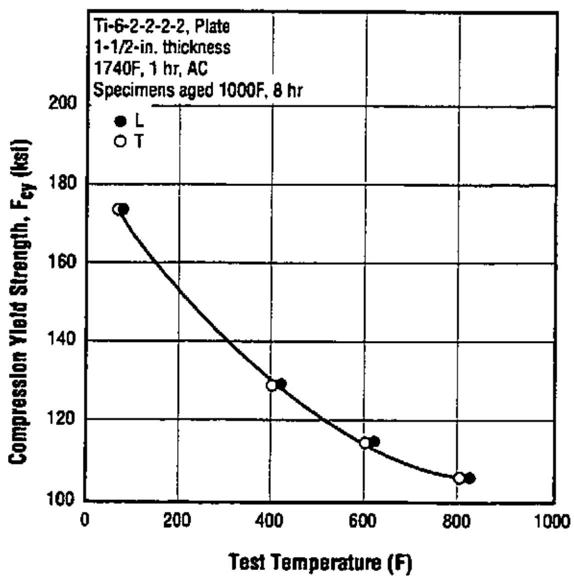

Fig. 3.3.2.5 Effect of temperature on the compression yield strength of conventionally processed plate (Ref. 8)

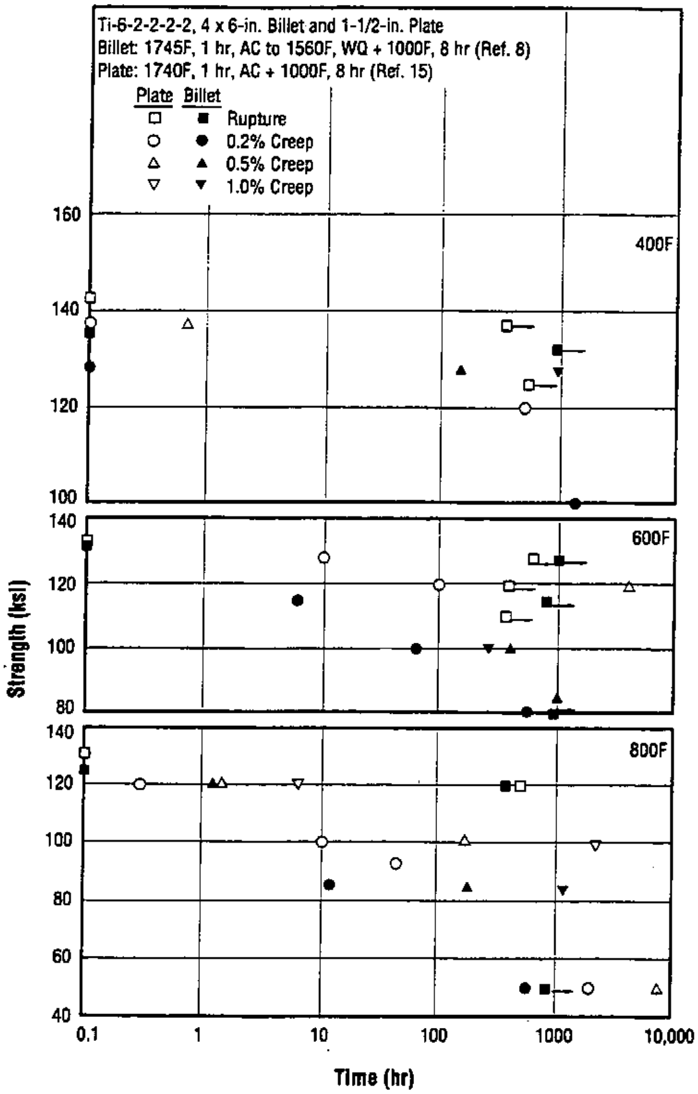

Fig. 3.4.1 Plastic creep and rupture data for conventionally processed plate and duplex annealed billet (Refs. 8, 15)

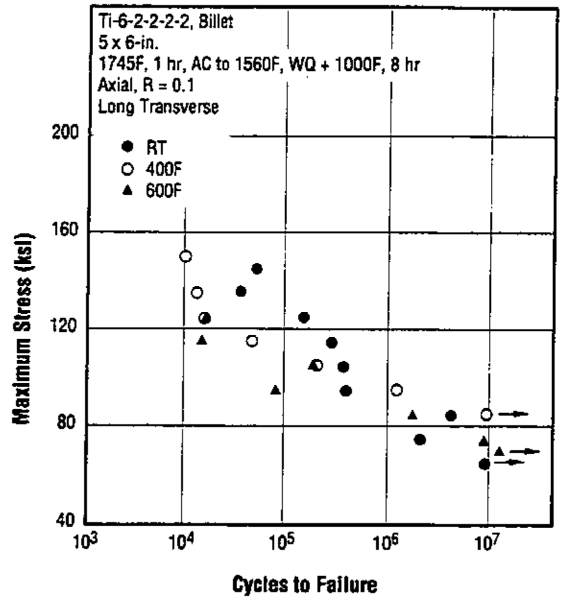

Fig. 3.5.1.1 Effect of test temperature on the smooth fatigue strength of conventionally processed billet (Ref. 15)

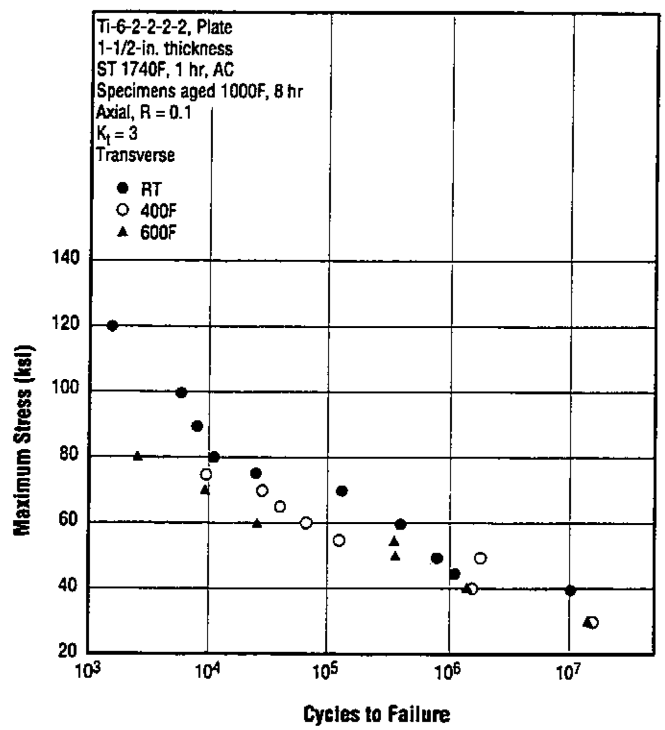

Fig. 3.5.1.2 Effect of test temperature on the notched fatigue strength of conventionally processed plate (Ref. 8)

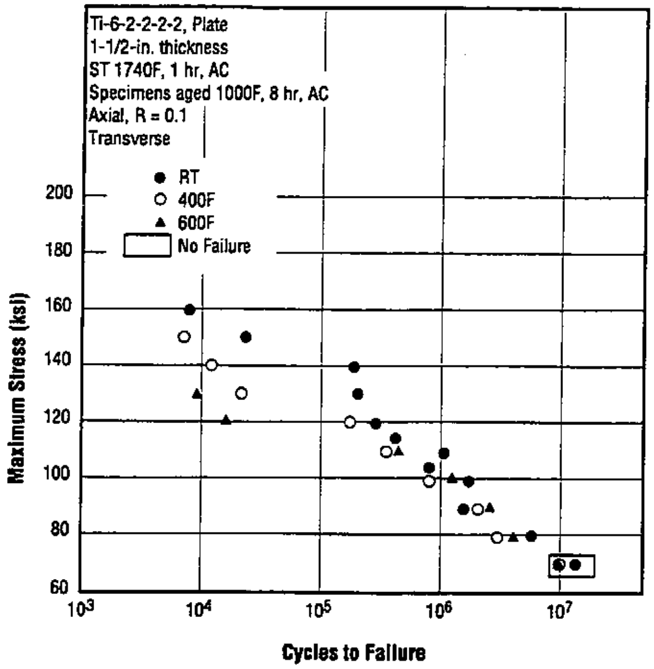

Fig. 3.5.1.3 Effect of test temperature on smooth fatigue strength of conventionally processed plate (Ref. 8)

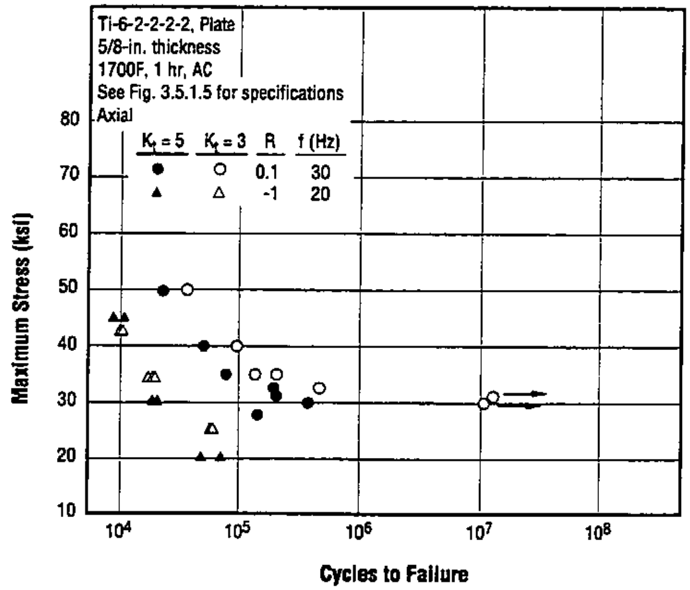

Fig. 3.5.1.4 Notch fatigue strength for conventionally processed solution treated unaged plate (Ref. 11)

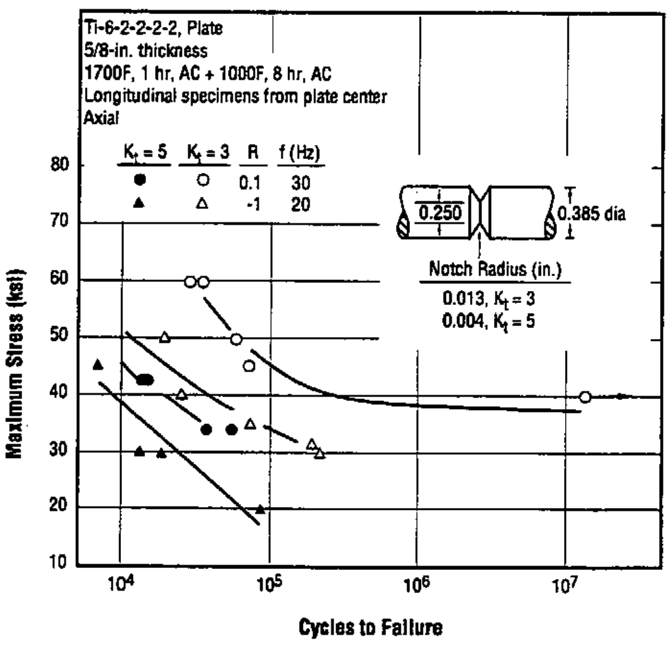

Fig. 3.5.1.5 Notch fatigue strength for conventionally processed plate (Ref. 11)

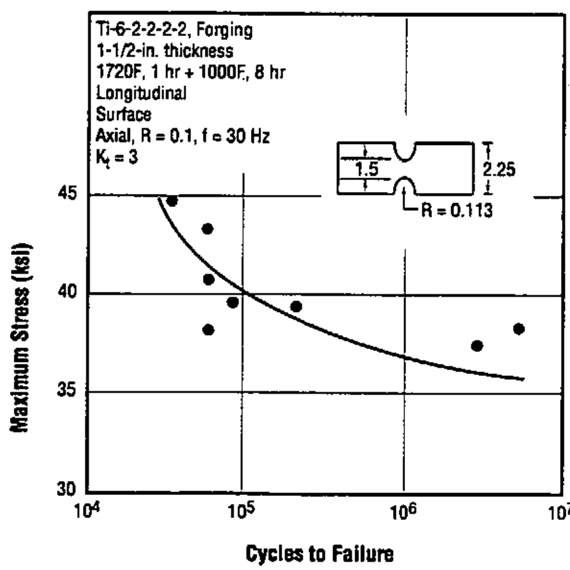

Fig. 3.5.1.6 Notch fatigue strength of a conventionally processed forging (Ref. 14)

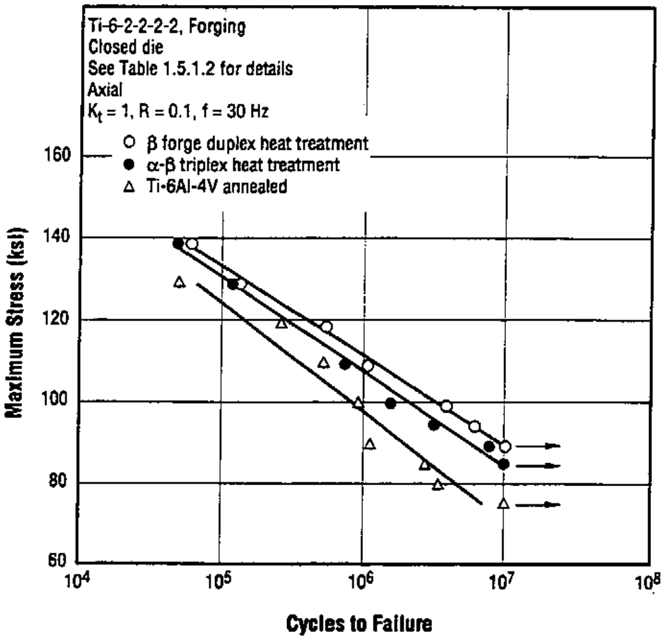

Fig. 3.5.1.7 Smooth fatigue strength produced by two thermomechanical processes applied to Ti-6-2-2-2-2 forgings compared with fatigue strength of annealed Ti-6Al-4V forgings (Ref. 6)

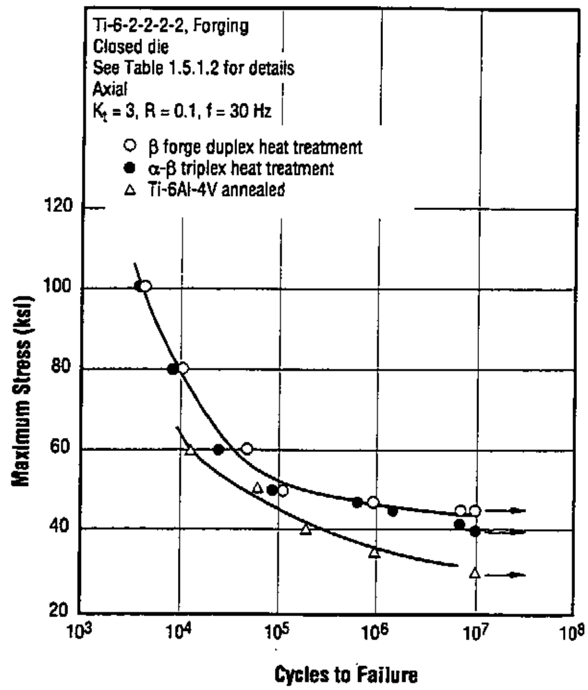

Fig. 3.5.1.8 Notch fatigue strength produced by two thermomechanical processes applied to Ti-6-2-2-2-2 forgings compared with fatigue strength of annealed Ti-6Al-4V forgings (Ref. 6)

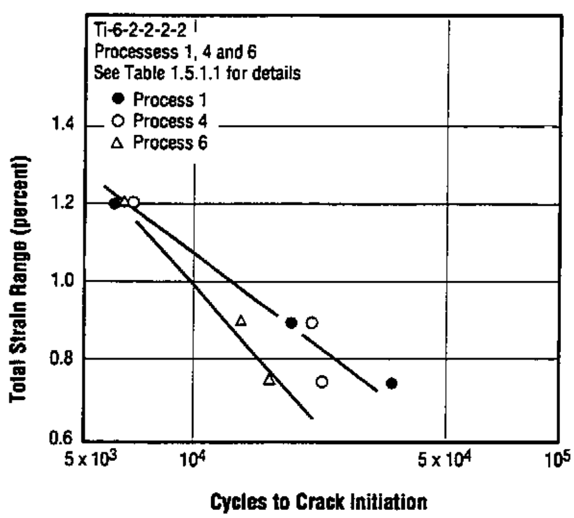

Fig. 3.5.2.1 Effect of thermomechanical processing on low cycle fatigue crack initiation of forgings (Refs. 4, 7)

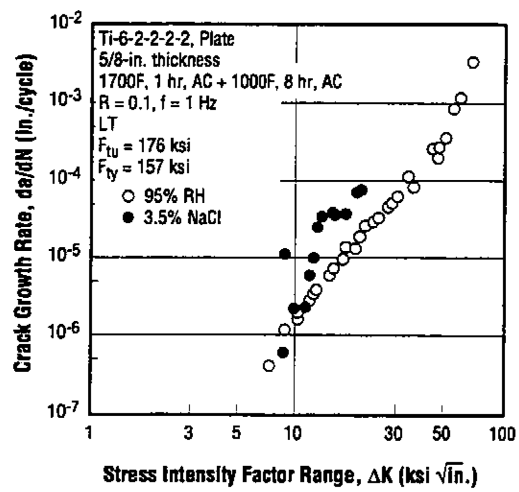

Fig. 3.5.3.1 Fatigue crack growth rates at 1 Hz for conventionally processed plate in humid air and in 3.5 percent NaCl (Refs. 10, 11)

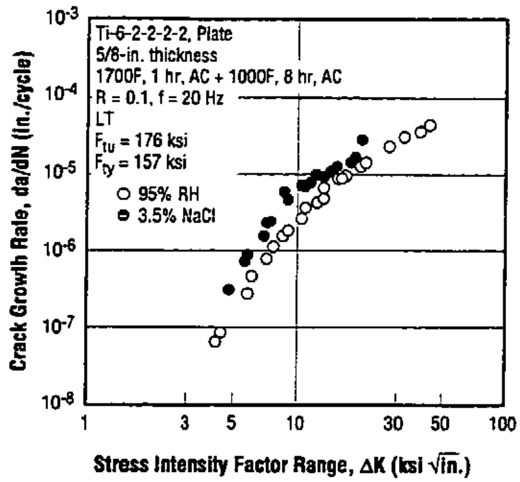

Fig. 3.5.3.2 Fatigue crack growth rates at 20 Hz for conventionally processed plate in humid air and in 3.5 percent NaCl (Refs. 10, 11)

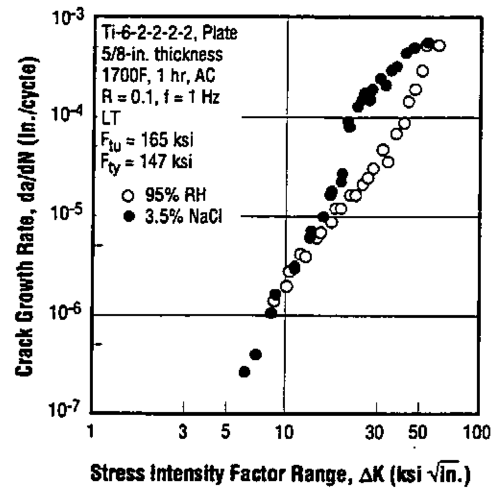

Fig. 3.5.3.3 Fatigue crack growth rates at 1 Hz for conventionally processed solution treated unaged plate in humid air and in 3.5 percent NaCl (Refs. 10, 11)

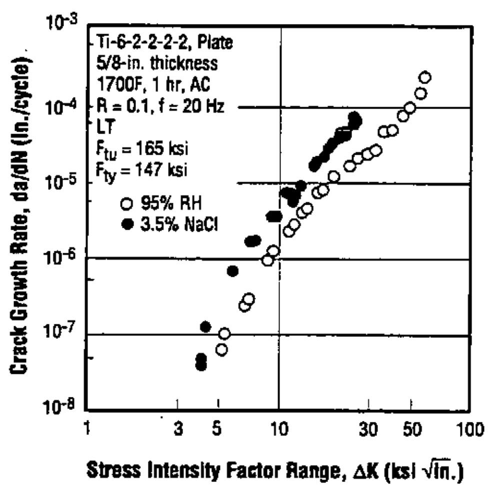

Fig. 3.5.3.4 Fatigue crack growth rates at 20 Hz for conventionally processed solution treated unaged plate in humid air and in 3.5 percent NaCl (Refs. 10, 11)

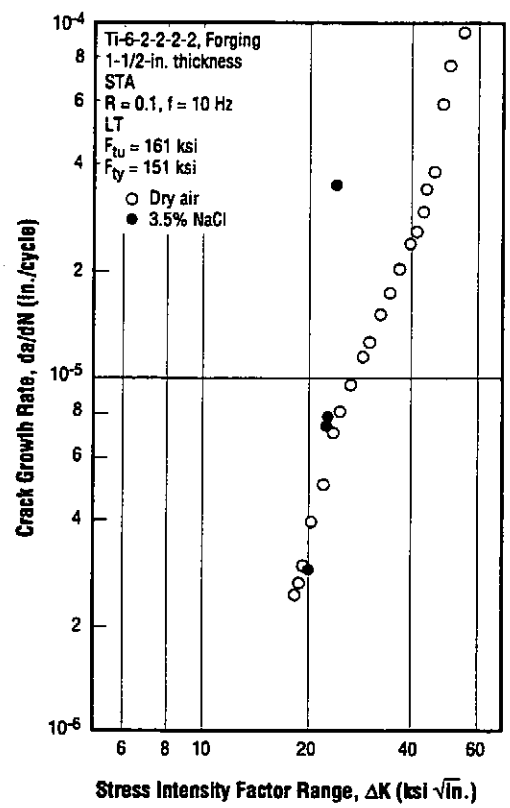

Fig. 3.5.3.5 Fatigue crack growth rates for conventionally processed forging in dry air and in 3.5 percent NaCl (Ref. 9)

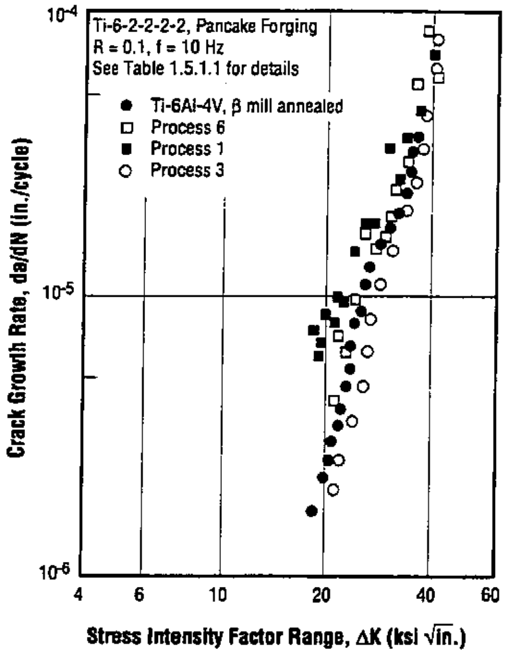

Fig. 3.5.3.6 Fatigue crack growth rates for Ti-6-2-2-2-2 forgings subjected to several thermomechanical processes compared with beta mill annealed Ti-6Al-4V forgings (Refs. 4, 7)

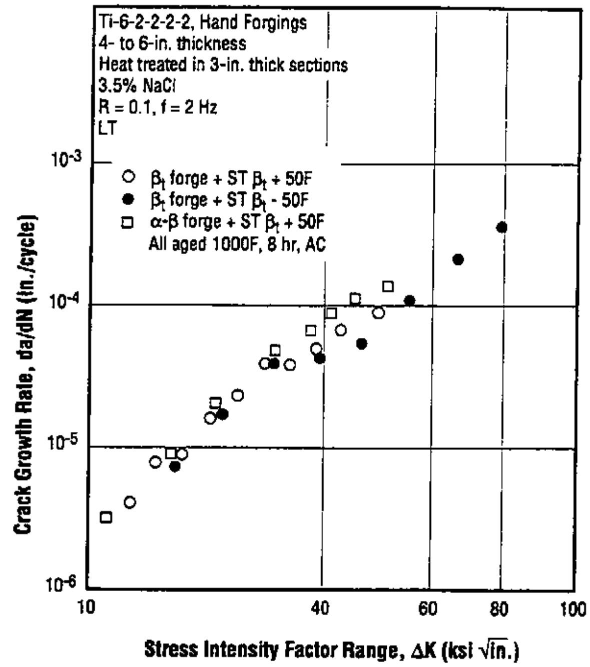

Fig. 3.5.3.7 Fatigue crack growth rates in 3.5 percent NaCl for hand forgings made from 8000-lb ingot and subjected to several thermomechanical processes (Ref. 20)

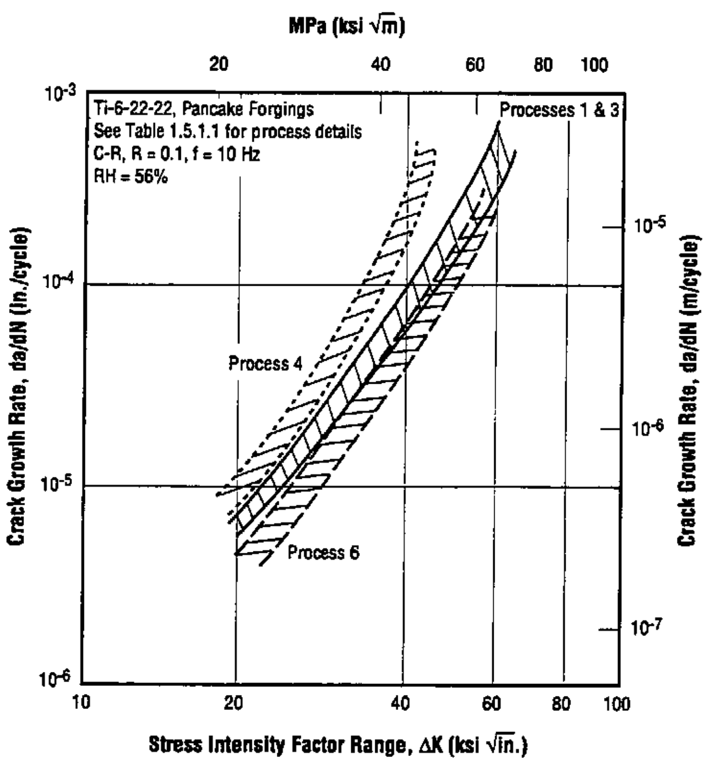

Fig. 3.5.3.8 Fatigue crack growth rates for forgings subjected to several thermomechanical processes (Ref. 4)

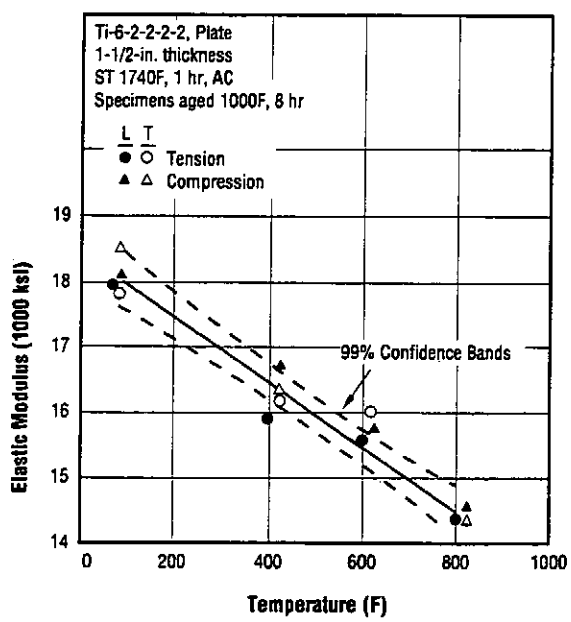

Fig. 3.6.2.1 Effect of temperature on the tension and compression elastic modulus of conventionally processed plate (Ref. 8)

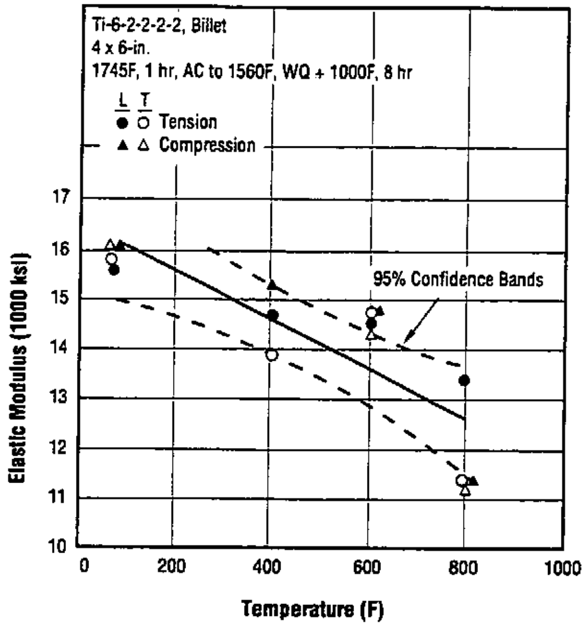

Fig. 3.6.2.2 Effect of temperature on the tension and compression elastic modulus of conventionally processed forged billet (Ref. 15)

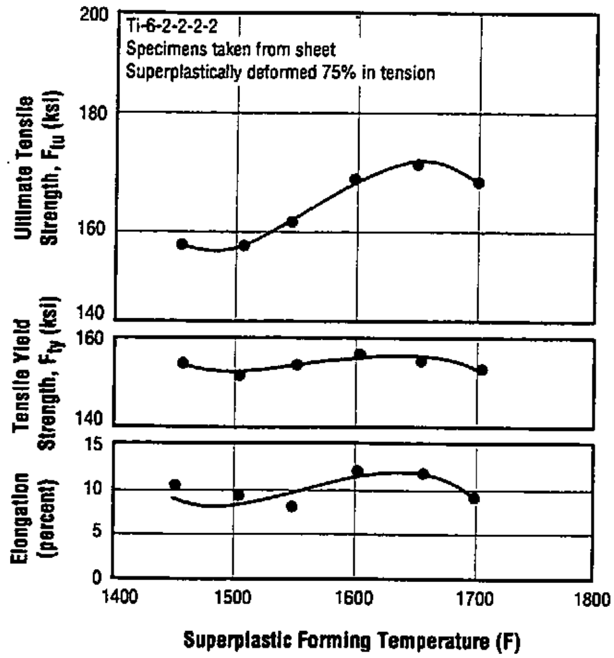

Fig. 4.1.2 Effect of superplastic forming temperature on the tensile properties of sheet (Ref. 19)

Table 4.3.1.1 Tensile properties and fracture toughness of electron beam welds in conventionally processed plate (Ref. 22)

Alloy	Ti-6Al-2-2-2-2 0.25Si, 0.12 Oxygen			
Form	0.625-in. Hot-Rolled Plate			
Condition	**ST 1725F, 1 hr, AC**		**ST 1750F, 1 hr, AC**	
Welding[a]	**No Weld + Age[b]**	**Weld + Age**	**No Weld + Age**	**Weld + Age**
F_{tu} (ksi)	182	180	180	178
F_{ty} (ksi)	156	166	165	164
e (percent)	13	17	17	17
RA (percent)	35	35	34	30
K_{Ic} (ksi $\sqrt{in.}$)[c]	44	_[d]	47	_[d]

[a] Electron beam welding parameters: beam current 300 ma, voltage 45 kV, energy input 20.4 kJ/inch, gun to work 8-inches. No filler metal.
[b] All specimens aged 1000F, 8 hours.
[c] CT specimens with crack at weld centerline.
[d] Specimens failed during fatigue cracking.

References

1. Product Bulletin: RMI Titanium Company, "RMI 6-22-22 High Strength Alloy for Light Weight Components."
2. "Mechanical Property Data Ti-6Al-2Zr-2Sn-2Mo-2Cr Alloy: Solution Treated and Aged Plate," AF33615-72-C-1280, Battelle-Columbus Laboratories (April 1973).
3. G. A. Bella, "Properties of Ti-6Al-2Sn-2Cr-2Mo-2Zr-0.25Si," RMI Titanium Company, Niles, OH (May 8, 1991).
4. A. K. Chakrabarti; R. Pishko; B. M. Sample; and G. W. Kuhlman, "TMP Conditions-Microstructure-Mechanical Property Relation Ti-6-2-2-2-2 Alloy," 7th International Titanium Conference, San Diego, CA (July 2, 1992).
5. G. W. Kuhlman; K. A. Rohde; and A. K. Chakrabarti, "Characterization of Ti-6-2-2-2-2 A High Strength Alpha-Beta Titanium Alloy for Fracture Critical Applications," *ibid.*
6. G. W. Kuhlman; A. K. Chakrabarti; and R. S. Beaumont, "Data Sheet on Beta Processed Titanium Alloy Ti-6Al-2Sn-2Zr-2Mo-2Cr+Si Forgings (Ti-6-2-2-2-2-S)," Alcoa Forging Division (March 15, 1991).
7. Personal Communication to W. F. Brown, Jr., from G. W. Kuhlman, Alcoa Forging Division.
8. O. L. Deel; P. E. Ruff; and H. Mindlin, "Engineering Data on New Aerospace Structural Materials," AF Contract F33615-72-C1280, Battelle-Columbus Laboratories, Technical Report, AFML TR-63-114 (June 1973).
9. R. R. Wells, "New Alloys for Advanced Metallic Fighter Wing Structures," AIAA Paper No. 74-372, *AIAA/ASME/SAE Structures, Structural Dynamics and Materials Conference,* Las Vegas, NV (April 17-19, 1974) (data from ref. 14).
10. Tabular Data received by J. E. Campbell of Battelle-Columbus from J. C. Frishette, Program Manager, USAF Lockheed Contract F33615-72-C-2165 (July 27, 1973).
11. *ibid*, from Lockheed-Georgia Company, Marietta, GA, (February 8, 1974) (see ref. 12).
12. C. R. Bigham, et al, "Advanced Metallic Structures: Cargo Wing Design, for Improved Cost, Weight and Integrity," Final Technical Report, July 1972 through July 1973, AFFDL-TR-73-51, AF Contract F33615-72-C2165, Lockheed-Georgia Company (June 1973).
13. "Collected Engineering Data Sheets (Air Force Data Sheet Program)," Final Report, April 1965 to September 1968, AFML-TR-78-179, Battelle-Columbus Laboratories (December 1978).
14 F. A. Figge; R. R. Wells; et al, "Advanced Metallic Structure; Air Superiority Fighter Wing Design for Improved Cost, Weight and Integrity," Vol. III Materials, Report AFFDL-TR-73-52 AF Contract F33615-72-C1891, Northrup Corporation (June 1973).
15. O. L. Deel; P. E. Ruff; and H. Mindlin, "Engineering Data on New Aerospace Materials," AFML-TR-75-97, AF Contract F33615-75-C5073, Battelle-Columbus Laboratories (June 1975).
16. R. A. Robinson, Boeing Document 5PD95006, Boeing Military Airplane Division (June 1994).
17. G. S. Hall; S. R. Seagle; and H. B. Bomberger, "Improvement in High Temperature Tensile and Creep Properties of Titanium Alloys," Titanium Science and Technology, *Proceedings of Second International Conference,* Eds. R. J. Jaffee and H. M. Burte, Vol. 4, p. 2141, Plenum Press, NY (1973).
18. S. R. Seagle; G. R. Seagle; and H. R. Bomberger, "Development of a Deep Hardenable Alloy for Intermediate Temperature Applications," *ibid*, Vol. 3, p. 1981.
19. R. C. Bliss, "Evaluation of Ti-6Al-2Sn-2Zr-2Cr-2Mo-0.23Si Sheet," *Titanium '92, Science and Technology,* Eds. F. H. Froes and I. Caplan, The Minerals, Metals and Materials Society, p. 201 (1993).
20. H. R. Phelps and J. R. Wood, "Correlation of Mechanical Properties and Microstructures of Ti-6Al-2Sn-2Zr-2Cr-2Mo-0.23Si Titanium Alloy," *ibid*, p. 1.
21. R. R. Boyer and A. E. Caddey, "The Properties of Ti-6Al-2Sn-2Zr-2Cr-2Mo-0.23Si Sheet," *ibid*, p. 1.
22. R. W. Messler, Jr., "Electron Beam Weldability of Advanced Titanium Alloys," *Welding Research,* Supplement to the Welding Journal (May 1981).
23. M. E. Mahoney and N. F. Paton, "Fatigue and Fracture Characteristics of Silicon-Bearing Titanium Alloys," *Metallurgical Transactions A*, Vol. 9A, p. 1497 (October 1978).
24. J. R. Wood and H. R. Phelps, "Effect of Silicon on Structure and Properties of Ti-6Al-2Sn-2Zr-2Cr-2Mo-Si," *Harold Margolin Symposium on Ti Alloys*, 1994 TMS Annual Meeting, San Francisco, CA.
25. J. A. Hauser; R. W. Judy; and T. W. Crooker, "Draft Standard Method of Test for Plane Strain Stress-Corrosion Cracking Resistance of Metallic Materials in Marine Environment," NRL Memo Report 5296 (March 22, 1984).
26. Personal Communication to W. F. Brown, Jr., from A. Ponte, ASC/YFFI, F-22 SPO, WPAFB, OH (November 14, 1994).
27. Personal Communication to W. F. Brown, Jr., from H. Phelps, Lockheed, F-22 Program (January 1995).
28. Personal Communication to W. F. Brown, Jr., from Margaret Tuttle, Boeing Military Airplane, F-22 Program, Seattle, WA (February 1995).

This page is blank.